UNIVERSITY OF CALIFORNIA, SAN DIEGO

Modulating cellular fate with arrayed cellular microenvironment technology

A Thesis submitted in partial satisfaction of the requirements
for the degree Master of Science

in

Bioengineering

by

Kevan Dinesh Shah

Committee in Charge:

Professor Shu Chien, Chair
Professor Karl Willert
Professor Shyni Varghese

2009

The Thesis of Kevan Dinesh Shah is approved and it is acceptable in quality and form for publication on microfilm and electronically:

Chair

University of California, San Diego

2009

TABLE OF CONTENTS

Signature Page iii

Table of Contents iv

Acknowledgements v

Abstract vi

Introduction 1

Human Embryonic Stem Cell Culture Conditions

- Introduction 3
- Results 4
- Discussion 11

Synthetic Polymers as Matrices for hESC Culture

- Introduction 16
- Results 17
- Discussion 19

RNA Interference

- Introduction 22
- Results 24
- Discussion 27

Conclusion 28

Materials and Methods 30

Appendix 36

References 57

ACKNOWLEDGEMENTS

I would like to thank Dr. Shu Chien for supporting me as a Chair of my thesis committee. I will always value his guidance and support for me throughout my experiences here.

I would also like to acknowledge Dr. Shyni Varghese for her kind assistance with my research. I am grateful for her willingness to discuss research despite her demanding schedule.

Dr. Karl Willert has also been a great mentor throughout my time here at UCSD. His advice and support has made my experience here an enriching and rewarding one.I would like to acknowledge Thomas Fellner, Megan Robinson, and ZoeVomberg from the UCSD Stem Cell Core for helping me quickly acclimate to working in a stem cell lab. They made my lab experience an enjoyable one, and it was a pleasure working with them.

Finally, I would like to extend my sincere gratitude to Dave Brafman for his immeasurable support. Without him, completion of my research would have taken twice as long. His guidance, encouragement, and assistance throughout my research efforts have undoubtedly enriched my research experiences and helped me immensely in my developing career.

In the appendix, figures 1, 2, 3, and 5 are reproductions from Brafman D, Shah K, Fellner T, Chien S, Willert K. Defining long-term maintenance conditions of human embryonic stem cells with arrayed cellular microenvironment technology. Stem Cells and Development, 2009 (In Press). The thesis author was the secondary author of this paper.

ABSTRACT OF THE THESIS

Modulating cellular fate with arrayed cellular microenvironment technology

by

Kevan Dinesh Shah

Master of Science in Bioengineering

University of California, San Diego, 2009

Professor Shu Chien, Chair

High throughput screening (HTS) methodologies allow for simplified analysis of numerous conditions. The development of the arrayed cellular microenvironment technology has allowed for multi-factorial investigations into cellular processes through controlling the cellular environment. Here, we describe the development of a HTS cellular microarray technology and its application to (1) the identification and analysis of an optimal, defined matrix composition for human embryonic stem cells

(hESCs), (2) the testing of synthetic polymers for their ability to support hESC growth, and (3) the development of a functional genomics screening platform. Through examination of gene expression of hESCs cultured on the defined matrix identified, we characterized maintenance of pluripotency and demonstrated differentiation potential. Additionally, polymers were systematically screened for ability to support hESC culture. Long-term culture methods on discovered polymers were examined through culture on hydrogels. Furthermore, we investigated a novel method of siRNA screening using this technology. The versatile arrayed cellular microenvironment technology can be utilized to understand the complex factors that modulate cellular activity and influence cell adherence, proliferation, and fate.

INTRODUCTION

In multi-cellular biological systems, the *in vivo* cellular microenvironment is crucial in determining cell fate and modulating cellular activity. This environment is defined by various components such as extracellular matrix (ECM), signaling molecules, and cell-cell interactions. Using current methods of cell culture, modeling these complex microenvironments *in vitro* requires large, painstaking, and costly approaches to test various combinations of the numerous signaling molecules and extracellular matrix components. The innovation of the arrayed cellular microenvironment technology has streamlined this screening process, and made it possible to discover specific conditions that are conducive for cell attachment, proliferation, and fate.

The arrayed cellular microenvironment technology was established by Flaim, *et al.* to spot ECM components onto a glass slide functionalized with an acrylamide hydrogel pad [1, 2]. This technology uses a DNA microarray spotter to place the ECM components on the glass slide. More specifically, ECM proteins are pipetted into a 384 well plate in various combinations and are deposited in an arrayed format onto the slide by the microarray spotter. These slides are then seeded globally with the cells of interest. Over the course of the following days, adhesion, growth, and morphology are monitored using microarray imagers and confocal microscopy. We have improved and expanded this technology, which we described in a recent publication [3]. In brief, we improved this technology platform by (1) increasing the number of conditions per slide, (2) incorporating soluble factors, such as growth factors, into the spotted microenvironments, (3) utilizing automated confocal microscopy for data acquisition,

and (4) developing new statistical analysis tools to rapidly process the data. Providing signaling molecules in the spots rather than in the liquid medium is a critical advance as it allows for greater throughput analyses of ECM protein and growth factor combinations.

In this thesis, I explore various applications of this arrayed cellular microenvironment technology and propose considerations for future investigation. First, long-term maintenance of pluripotency is analyzed in human embryonic stem cells (hESCs) in conditions previously defined using this technology. Next, the arrays are used to screen various polymers to study their effects on cell attachment, growth, and fate. I conclude with an investigation into RNA interference screening capabilities on this array format. The arrayed cellular microenvironment technology is a unique innovation that can be applied to a diverse range of experiments, as I depict throughout this paper below.

Figure 1 is a reproduction from Brafman D, Shah K, Fellner T, Chien S, Willert K. Defining long-term maintenance conditions of human embryonic stem cells with arrayed cellular microenvironment technology. Stem Cells and Development, 2009 (In Press). The thesis author was the secondary author of this paper.

HUMAN EMBRYONIC STEM CELL CULTURE CONDITIONS

Introduction

Human embryonic stem cells (hESCs) have the ability to differentiate into every cell type in the body. They can also be grown without differentiation (i.e. self-renew), thereby creating a large supply of cells, which can then be differentiated into a cell type of choice. Thus, hESCs provide a cellular "raw" material that can be potentially used for *in vitro* analyses of many difficult-to-grow primary cell types. In addition, these cells hold promise for future regenerative medicine therapies, drug discovery and disease modeling. Since the first successful isolation and propagation of hESCs in 1998 by Dr. J. Thomson's laboratory [4], many researchers have studied culture conditions for hESCs. Currently, a common method of culturing hESCs involves seeding cells on top of a layer of feeder cells (which are of human or mouse origin- most frequently Mouse Embryonic Fibroblasts or MEFs). This feeder layer provides the stem cells a suitable matrix and appropriate signals to retain their pluripotency [5]. In recent years, researchers have identified methods of hESC culture that do not involve feeder layers, such as Matrigel^{TM} (BD) [6]. Along with these substrates that support attachment of hESCs, Mouse Embryonic Fibroblast conditioned media (MEF-CM, or CM) is a commonly used medium to feed cells.

However, all conditions developed to date to grow hESCs in an undifferentiated state are comprised of undefined components. These components contaminate hESCs with immunogenic animal products [7], and therefore cannot be used in future stem cell-based treatments in humans. Currently, most studies have focused on non-immunogenic medium replacements [8-15], while only few have

focused on replacing Matrigel with human feeder-free substrates [16-20]. The studies that have centered on substrate replacement have used various Extracellular Matrix Proteins (ECMPs), which have been found to affect stem cell cultures [21, 22], but have not been methodically studied.

In the section below, we expand on a recent publication where we systematically investigated the effects of various ECMPs on hESC proliferation and maintenance of pluripotency [3]. Furthering this analysis, we developed and implemented a quantitative PCR assay for measuring pluripotency in hESCs grown on a defined matrix (an optimal combination of ECMPs discovered in Brafman *et al.*). Also, we examined differentiation potential by characterizing gene expression of embryoid bodies created from cells grown on this defined matrix.

Results

Microarray screening to establish defined matrix for hESC growth

Through work with the arrayed cellular microenvironment technology spearheaded by Dave Brafman, we established optimal defined conditions for proliferation and maintenance of pluripotency of hESCs [3]. As described below, our experimentation revealed that these conditions consisted of a combination of various extracellular matrix proteins (ECMPs); more specifically, collagen I, collagen IV, fibronectin, and laminin (C1+C4+Fn+Ln).

We began the study with analysis of six ECMPs (C1, collagen III [C3], C4, collagen V [C5], Fn, and Ln) as substrates for hESC growth. After spotting these proteins individually at various concentrations onto glass slides and seeding with two cell lines (Hues 1 and Hues 9), we fixed and stained the adherent cells with a DNA

stain to assess for proliferation. It became evident that each ECMP differentially supported hESC proliferation, with varying results depending on the cell line. Overall, the results illustrated that individual ECMPs were not optimal for hESC growth [3]. We then proceeded to spot all combinations of the six ECMPs mentioned above (n=63) along with Matrigel as a control. Once again we stained for DNA to measure proliferation and imaged the spots after 5 days. To analyze these spots, the intensity of the signal was converted to a color heat map was created with green indicating a decrease and red indicating an increase in proliferation relative to the global mean (Fig 2a). Using Pearson correlation as a similarity metric for $\log_2$ of the DNA signal, four main clusters were identified: 1) high proliferation and in Hues 1 and Hues 9 (red cluster), 2) high proliferation in only Hues 9 (blue cluster), 3) high proliferation in only Hues 1 (orange cluster), 4) low proliferation for both Hues 1 and Hues 9 (green cluster). We also created a Z-score for each combination (titled Proliferation Index in Brafman, *et al.*) using the $\log_2$ of DNA signals and plotted the results, which demonstrate the same trends as seen in the heat map (Fig 2b). Images of representative spots for each of the four groups are depicted in Figure 2c. These results established that combinations of ECMPs were suitably better than individual ECMPs at supporting hESC proliferation.

In order to examine substrate effects on maintenance of pluripotency, we again spotted slides with 63 combinations of ECMPs, and seeded the arrays with Hues 9 cells. After 5 days, we fixed and stained with either Oct4 or Nanog, two markers that have been proven to be upregulated in undifferentiated hESCs and quickly downregulated once cells differentiate [5, 23]. We also stained for DNA using a

Hoechst stain. After staining, we imaged the slides and analyzed expression of Oct4 or Nanog. A ratio was developed to normalize expression of Oct4 or Nanog to total cell number, which is represented by the DNA stain. This ratio of pluripotency was plotted in a heat map alongside proliferation values (Fig. 3a). In this heat map, four clusters are evident: 1) high proliferation and high maintenance of pluripotency (red cluster), 2) low proliferation and high maintenance of pluripotency (blue cluster), 3) high proliferation and low maintenance of pluripotency (orange cluster), 4) low proliferation and low maintenance of pluripotency (green cluster).

Using this pluripotency ratio, we created a Z-score for pluripotency (titled Pluripotency Index in Brafman, *et al.*), and plotted the resulting data against the Z-score for proliferation (Fig. 3b). In this figure, four clusters that correlate to those seen in the heat map are evident. In Figure 3c, representative spots from each of the four clusters are depicted. After observing the positive proliferation and pluripotency Z-scores, it became clear that the combination of collagen I, collagen IV, fibronectin and laminin (C1+C4+Fn+Ln) ranks near the highest of both statistical markers. Thus, according to our cellular microarray screen, this matrix of C1+C4+Fn+Ln is the optimal combination of ECMPs for supporting hESC proliferation and maintenance of pluripotency. To verify our findings, we cultured hESC in a larger, more traditional format on the defined matrix of C1+C4+Fn+Ln at a concentration of 10 $\mu g/cm^2$. After 10 passages on this defined matrix, we confirmed that cells remained karyotypically normal and established their pluripotency through immunostaining and quantitative PCR (qPCR) of undifferentiated and *in vitro* differentiated cells [3]. In this paper, we

focus on using qPCR to characterize the pluripotency of the hESCs grown on the defined matrix of C1+C4+Fn+Ln.

Establishment of quantitative PCR assay for analyzing pluripotency in hESCs

In order to effectively determine maintenance of pluripotency in hESCs, we needed to develop an assay that could measure mRNA levels of pluripotency markers in hESCs. To accomplish this, we began with RNA isolation and continued to quantitative PCR. First, we isolated RNA using TRIzol (Invitrogen), and confirmed RNA integrity by gel electrophoresis (Fig. 4a), which revealed the characteristic 18S and 28S ribosomal RNA species [24]. RNA was converted to cDNA by reverse transcription prior to quantitative PCR using TaqMan (Applied Biosystems) primers for Oct4 and Nanog. To effectively measure maintenance of pluripotency, we performed a simple experiment where we grew stem cells over 4 days with and without MEF Conditioned Medium (CM). As hESCs grown without CM undergo morphological changes and tend to differentiate [15], we hypothesized that this change would be accompanied by a reduction in gene expression of known markers of the pluripotent state, POU5F1 (Oct4) [25] and Nanog [26]. Thus, we performed quantitative PCR using these markers to measure changes in gene expression over 4 days with and without CM (Fig. 4b). By day 4, the hESCs grown without CM have a significant reduction in both Oct4 and Nanog levels relative to cells in the presence of CM. This indicates that the hESCs grown without CM do not maintain expression of pluripotency markers as well as those grown in CM, and demonstrates the sensitivity and efficacy of qPCR as a method to assess the pluripotent state.

Utilizing quantitative PCR for hESC pluripotency analysis

In Brafman, *et al.*, my efforts focused on establishing that these defined conditions (C1+C4+Fn+Ln) could support long term maintenance of pluripotency through quantitative PCR analysis. Since previous research has established Matrigel to be a good substrate for feeder-free growth [27], we analyzed Oct4 and Nanog signals of Hues 9 and H9 cells at passage 10 compared to the same cell types grown on Matrigel at passage 10 (Fig. 5, [3]). In this figure, we can determine that the relative Nanog and Oct4 expression in both Hues 9 and H9 cells are either equivalent or higher in the defined matrix conditions using conditioned medium than in Matrigel. We also examined the defined StemPro medium (Invitrogen), yielding similar results. The relative quantities of Nanog are slightly higher than in Matrigel in both cell types, and Oct4 signals vary from higher in H9s to lower in Hues 9s.

This previous result established that our defined conditions supported hESC pluripotency at passage 10. However, we did not monitor changes in Oct4 and Nanog levels in hESCs through multiple passages, thus reducing the significance of the data. To further this analysis and confirm our results, we ran a long-term quantitative PCR assay to monitor gene expression of hESCs grown on the defined matrix. The hESCs were compared to Matrigel through five passages. Using two cell lines, H9 and Hues 9, we analyzed Oct4 and Nanog expression on four different combinations of substrates and media: 1) C1+C4+Fn+Ln + MEF Conditioned Media (CM), 2) C1+C4+Fn+Ln + StemPro (Invitrogen), 3) Matrigel + StemPro, and 4) Matrigel + CM, which served as our control (Fig. 6). Figure 6 shows that these two stem cell lines grown on the defined matrix express pluripotency genes Oct4 and Nanog at equivalent or higher levels than Matrigel in Conditioned Medium, suggesting that the defined

matrix of C1+C4+Fn+Ln is a superior replacement for maintaining pluripotency of hESCs. An exception to this is the relative Nanog expression in passage 4 of the Hues 9 cell line, which will be further discussed below. In StemPro medium, the Oct4 and Nanog levels in hESCs are roughly equivalent to cells grown in Matrigel + CM, and correlate with hESCs grown in Matrigel + StemPro.

Analyzing ECMP concentration effects on pluripotency

Following this result, we moved forward to examine gene expression of stem cells grown on lower concentrations of our defined matrix. We chose to experiment with a different human embryonic cell line, Hues 1, to illustrate the versatility of the C1+C4+Fn+Ln matrix while analyzing the effects of concentration on Oct4 and Nanog expression. Three different concentrations of the defined matrix were used: 10 $\mu g/cm^2$ (our previous standard), 5 $\mu g/cm^2$, and 2.5 $\mu g/cm^2$. Cells were not able to be cultured for 5 passages on the 2.5 $\mu g/cm^2$ concentration of ECMPs without significant morphological changes. Therefore, we proceeded with the 10 $\mu g/cm^2$ and 5 $\mu g/cm^2$ concentrations and isolated RNA through 8 passages grown on each concentration. We then performed qPCR and analyzed Oct4 and Nanog gene expression through all 8 passages (Fig. 7). We found that hESCs grown on the 5 $\mu g/cm^2$ display levels of Oct4 and Nanog slightly higher than Matrigel, suggesting that a reduction in ECMP concentration to 5 $\mu g/cm^2$ is adequate for maintenance of pluripotency in hESCs.

Characterizing embryoid bodies using TaqMan Low Density Arrays (TLDA)

In order to further our analysis of gene expression in hESCs, we utilized TaqMan Low Density Arrays (Applied Biosystems), which allow for quantitative PCR testing of 96 genes per sample (90 genes + 6 endogenous controls). The Human Stem

Cell Pluripotency Array contains various pluripotency and lineage-specific differentiation markers, thus giving us further insight into hESC gene expression. To confirm pluripotency and differentiation potential of hESC lines cultured on the defined matrix, we differentiated hESCs in vitro using an embryoid body formation (EB) assay. First, we created 3-week (spin) embryoid bodies from undifferentiated hESCs grown on the defined matrix for 10 passages (Fig. 8). In order to do this, we transferred cells into an untreated, v-bottom 96 well plate, then centrifuged and incubated overnight (Step 1). To form EBs, cell aggregates were pipetted into an ultra-low binding 6 well plate and incubated for a week (Step 2). After this, we transferred the embryoid bodies to Matrigel-coated plates for two weeks to allow the EBs to grow (Step 3). After this 3-week differentiation process, RNA was isolated from the EBs and gene expression profiles were assessed using the TaqMan arrays. Undifferentiated hESCs were used as a calibrator.

To analyze the qPCR data, $\log_{10}$ of the fold change, or relative quantity (RQ), values from 3 replicates were displayed in a heat map (Fig. 9). The clustering analysis for the rows and the columns was done using Pearson correlation, with red depicting increased expression of genes in the EBs relative to undifferentiated hESCs, and green depicting decreased expression. A cluster of highly expressed genes is visible in the heat map, identified by the boxed red cluster in Figure 9. This cluster contains multiple lineage-specific genes (Endoderm: LAMA1, FN1, SST; Ectoderm: SYP, PAX6, PECAM; Mesoderm: COL1A1, COL2A1, WT1; Trophoblast: EOMES), suggesting that cells within the EBs are spontaneously differentiating into various cell types. However, there are also a few stemness markers upregulated in the EBs

(COMMD3, NOG, IL6ST, CRAB, NR6A1, KIT), indicating that the cell population within the EBs is heterogeneous and likely includes some undifferentiated stem cells. This upregulation in EBs of markers normally associated with undifferentiated hESCs has also been observed in previous studies [23]. In the heat map, there is also a cluster of genes that is significantly downregulated in EBs in comparison to undifferentiated hESCs (Fig. 9, boxed green cluster). These downregulated genes are clearly associated with the stem cell state, consisting of pluripotency markers (POU5F1 [Oct4], NANOG, TDGF1, GABRB3, DNMT3B) and stemness markers (IFITM1, IFITM2, UTF1, GRB7, EBAF, GAL, FGF4, PODXL, ZFP42, SEMA3A, LEFTB, CD9, NR5A2). Consequently, this result demonstrates that embryoid bodies generated from undifferentiated hESCs grown on the defined matrix have gene expression profiles consistent with typical EBs. There is an upregulation of lineage-specific genes and downregulation of markers associated with the pluripotent stem cell state.

Discussion

Quantitative PCR assay for maintenance of pluripotency on defined matrix

Utilizing quantitative PCR, we established an assay for characterizing maintenance of pluripotency in human embryonic stem cells and used this assay to demonstrate the potential of the defined matrix established by Brafman, *et al* [3]. In Figure 4, we establish the use of qPCR for the detection of hESC differentiation: when hESCs are cultured for 4 days in the absence of CM, we observe a 5-fold decrease in Oct4 and a 6-fold decrease in Nanog expression. This significant downregulation of pluripotency markers helps us understand the expression levels in the defined matrix-Matrigel comparisons demonstrated in Figures 6 and 7. For most cases, the pluripotent

marker gene expression levels of cells grown on the defined matrix in CM are consistently similar to or greater than of cells grown on Matrigel. At no point do the Oct4 or Nanog levels decline more than 2-fold in conditioned medium. Furthermore, Oct4 and Nanog signals of hESCs grown on Matrigel itself vary from passage to passage, as demonstrated in Figure 10. In Figure 10 we reproduce the qPCR data seen as in Figure 6, but instead of using each Matrigel passage as a calibrator, we calibrate by passage 1 of Matrigel + CM. Here we see that Oct4 and Nanog levels of cells grown on Matrigel vary up to 3-4 fold. This indicates that even in the few cases where there was a slight decrease in expression of pluripotent markers in cells grown on the defined matrix compared to Matrigel, the gene expression levels observed on cells grown on the defined matrix are within a satisfactory range. In StemPro medium, the Oct4 and Nanog signals of hESCs grown on the defined matrix correlate well with hESCs grown on Matrigel. In the few cases where a greater than 2-fold decrease in expression compared to Matrigel + CM is noted (Fig. 6 H9 Oct4) in defined matrix + StemPro, this downregulation is also observed in Matrigel + StemPro. In general, the defined matrix outperforms Matrigel as a substrate when solely observing levels of pluripotent markers Oct4 and Nanog in conditioned medium. Although quantitative PCR data cannot be used independently to draw conclusions about maintenance of pluripotency in hESCs, this data supports the conclusions drawn in Brafman, *et al.* [3] and further characterizes the capability of the defined matrix of Collagen 1, Collagen 4, Fibronectin, and Laminin (C1+C4+Ln+Fn) in supporting hESC culture.

Maintenance of pluripotency in reduced concentration of defined matrix

In Figure 7, it is evident that Oct4 signals are elevated in cells grown on both 10 μg/cm^2 and 5 μg/cm^{2}of the defined matrix in comparison to Matrigel in the Hues 1 cell line. This elevation of signal is exaggerated due to fluctuating Oct4 and Nanog expression in hESCs grown on Matrigel as described above and illustrated in Figure 10. However, there is still an approximate 3-4 fold upregulation of Oct4 signal in cells grown on defined matrix + CM in comparison to Matrigel + CM. This elevation could be due to various causes, including: 1) culture on Matrigel suppresses Oct4 expression on the Hues 1 cell line, 2) the Hues 1 cell line responds to the defined matrix differently than the Hues 9 and H9 cell lines, 3) experimental variation. Further experimentation must be done to identify the cause of this effect. In contrast, Nanog signals in hESCs grown on the defined matrix + CM do not vary over 2-fold in relation to hESCs grown on Matrigel + CM, suggesting that substrate performance is equivalent. From this data it is evident that differences between cells grown on 5 μg/cm^2 and 10 μg/cm^2 concentrations of defined matrix are minimal; Oct4 and Nanog expression in both cases remain within 2-fold of each other. Even in the case of the single exception (Fig. 7, Oct4 levels in P7 and P8), the Oct4 signals are fluctuating within the same range, suggesting similarity. This indicates that a reduction in concentration of the defined matrix to 5 μg/cm^2 would have little to no effect on expression of pluripotency markers in hESCs.

Embryoid body characterization through TLDA plates

Through the TaqMan Low Density Arrays, we were able to analyze gene expression of 90 genes in embryoid bodies differentiated from hESCs grown on the defined matrix. Through this analysis we observed that EBs expressed lineage specific

markers while downregulating markers of pluripotency (Fig. 9- red denotes upregulation & green denotes downregulation). To demonstrate this distinct profile of gene expression in embryoid bodies, we created charts of differentiation genes upregulated and stemness genes upregulated (on average) in the EBs (Fig. 11). In these charts it becomes evident that a majority of differentiation genes are upregulated (72%, 36/50) while a minority of genes associated with the stem cell state are upregulated (26.5%, 11/40, Fig. 11a). To further this analysis, we created a figure to characterize the breakdown of genes with increased expression in the embryoid body (Fig. 11b-c). In this figure, we see that 69% of Ectoderm, 67% of Mesoderm, 72% of Endoderm, and 100% of Trophoblast genes on the TaqMan array are upregulated in the EBs, suggesting that spontaneous differentiation occurred. Notably, none of the pluripotency markers (0/7) are upregulated. Furthermore, 6 out of 7 of these pluripotency markers are downregulated by 10-fold or more (POU5F1 [Oct4], NANOG, SOX2, DNMT3B, GABRB3, and TDGF1). This confirms that embryoid bodies do not maintain the pluripotent state of undifferentiated hESCs. However, a few of the Stemness markers are upregulated (33%, 11/33), possibly indicating that the cell population in the embryoid bodies could be heterogeneous and contain some undifferentiated hESCs (also observed by previous researchers [23]). Overall, analysis of the embryoid bodies using the TaqMan Low Density Arrays demonstrates the significant differences in gene expression of EBs relative to undifferentiated hESCs. This is demonstrated through upregulation of various early differentiation markers and downregulation of markers associated with pluripotency. This result confirms that hESCs cultured on the defined matrix of C1+C4+Fn+Ln have the capacity to

differentiate into various lineages. These cells retain their pluripotency while using the defined matrix as a substrate for culture.

As outlined above, we further characterized the defined matrix established by Brafman, *et al* [3]. Through the use of quantitative PCR, we were able to demonstrate that hESCs grown on a defined matrix (C1+C4+Fn+Ln) maintained equivalent expression of pluripotency genes as Matrigel, the current gold standard of feeder-free culture. These results support the conclusions drawn in Brafman, *et al.*[3]; this defined matrix is a capable substrate for feeder free culture of human embryonic stem cells.

Figures 2, 3, and 5 are reproductions from Brafman D, Shah K, Fellner T, Chien S, Willert K. Defining long-term maintenance conditions of human embryonic stem cells with arrayed cellular microenvironment technology. Stem Cells and Development, 2009 (In Press). The thesis author was the secondary author of this paper.

SYNTHETIC POLYMERS AS MATRICES FOR hESC CULTURE

Introduction

Human embryonic stem cell culture remains a costly and complex task, relying on a variety of biological substrates including extracellular matrix deposited by MEF or human feeder cell layers, and other animal-derived products such as Matrigel. These biological substrates can transmit diseases and non-human contaminants to the hESCs, thereby limiting the potential for clinical application. In addition, since biological systems have an inherent variability, chemical signals received from the substrates may vary. This can cause disparities in cells grown in the same culture conditions. These issues can be avoided through the use of a combination of purified extracellular matrix proteins (ECMPs) that would remove the disparities in signaling seen in MEFs or Matrigel. This is the solution proposed in Brafman, *et al.*, where a defined matrix that supports hESC culture was discovered [3]. Even with the identification of a defined matrix, however, the cost of cell culture is still a concern. Purified human ECMPs can range from approximately \$5-\$350 for 0.5 mg[1], which makes the costs of stem cell culture on the defined matrix significantly higher than culturing on MEFs or Matrigel. In order to reduce the costs associated with culture on defined substrates, we used this arrayed cellular microenvironment technology to screen various polymers and characterize their ability to support stem cell proliferation and pluripotency.

While analyzing synthetic polymer alternatives for cell culture, it is important to take into consideration that substrates that support cell growth also influence

[1]Referring to Sigma Human Collagen I, Collagen IV, Fibronectin, and Laminin prices as of 2/23/09

cellular activity [28, 29]. These substrates have a variety of properties that play a role in modulating cell activity, including surface morphology, hydrophobicity, and direct cell-substrate interactions [30]. Surface morphology in particular has been demonstrated to affect "cell function, shape, cytoskeletal tension, and regulatory pathways" [31] (also [32-35]). Currently, there is no established set of principles or properties that predict of which polymers would be satisfactory for supporting cell culture [30]. Thus, the importance for high throughput screening (HTS) cannot be understated in analyzing whether or not various polymers support cell attachment, proliferation and fate. In the following section, I describe the use of the arrayed cellular microenvironment technology to investigate synthetic polymers as substrates for hESC culture.

Results

Polymer Screens on Array Platform

To identify polymers suitable for supporting cell culture, we screened 43 polymers on the array platform. The polymers were either purchased (n=33) or synthesized (n=10, by Dr. Shyni Varghese). Polymers were dissolved in DMSO (4 mg/ml, % w/v), and spotted onto glass slides functionalized with acrylamide gel pads (Fig 12). Similar to the ECMP spotting procedure, we silanized a glass slide and coated it with an acrylamide gel pad. We then proceeded to spot our polymers onto these slides using a microarray printer. Initially, the spotted polymers were tested with an adherent H1299-CMV-GFP cell line. After seeding these cells globally, we observed cell attachment and proliferation after 3 days, and captured the cell growth data as described in the previous section. A total of 12 polymers were found to support

H1299 adherence and proliferation. Images of the polymer spots that successfully supported H1299 adherence and growth are shown in Figure 13.

After identifying a subset of polymers that supported H1299 cell attachment and proliferation, we seeded these polymer arrays with hESCs. After 6 days, we imaged cells on the polymer arrays (Fig. 14). Of the 12 polymers that supported H1299 growth, we found that only three different polymers were capable of supporting hESCs: Polymer #8, Polymer #12, and Polymer #24.

Long term culture of hESCs on polymer hydrogels

In order to analyze the long-term hESC culture potential of these polymers, we cultured hESCs on polymers in a larger, more traditional format. To this end, we created hydrogels using monomers of the polymers that were able to support hESC attachment and proliferation on the arrays. We were able to obtain 2 out of the 3 monomers that were successful on at retaining hESC on the spots: Polymer #12 and Polymer #24. To create these hydrogels, we began with testing monomer and bis-acrylamide (bis-AM) crosslinker concentrations used in acrylamide gels (10% monomer and .55% crosslinker). Monomer #12 hydrogels were successfully formed at this concentration, but Monomer #8 hydrogels were not able to be formed into proper gels. We proceeded to test various concentrations of Monomer #8 and bis-AM crosslinker in all combinations: 5%, 10%, 20%, and 30% Monomer #8 with 0.55%, 1%, 2%, and 3% bis-AM. Out of these 16 combinations, we were able to successfully form an optimal hydrogel at 10% monomer #8 and 1% bis-AM. This is the combination we utilized going forward.

After hydrogel formation and prior to cell seeding, we manipulated the hydrogels in one of two ways: either we dehydrated the hydrogels on a slide warmer, or we rinsed the hydrogels in ethanol and kept them in a PBS solution with antibiotics. We found that only the slides that had been dehydrated were able to support hESC attachment and proliferation. Since dehydration of hydrogels changes their surface morphology and mechanical properties, this result suggested that surface topology may be a critical factor for culturing cells on hydrogels.

Through 4 passages, we maintained the Oct4 GFP hESCs on Polymer #8 and #12 hydrogels (Fig 15). The cells on both polymers displayed a strong GFP signal, indicating that they have maintained their pluripotency. However, hESCs did not consistently attach and grow on the hydrogels; on each glass slide, cells seemed to attach and proliferate differently. At this time the source of this variability is unknown, but we speculate that the surface morphology is playing a greater role than we initially hypothesized.

Discussion

Through screening of 43 polymers on the arrayed cellular microenvironment technology, we were able to identify polymers that support hESC attachment and proliferation. This microarray screen helped us discover polymers in an efficient manner. This process would have taken much more time, effort and resources if traditional cell culture formats were used. The primary screen of H1299 cells acted as a positive control, ensuring that polymers were spotted successfully and that cells were supported by a subset of those spotted. Similarly to ECMPs [3], the spots that were successful in acting as a substrate for hESCs were also successful in the more common

cell line – H1299s in this case (HEK-293s in [3]). This fact indicates that hESCs are more selective than common cell types in substrate requirements, but do share some properties. This may be related to the observation that, unlike HEK-293 or H1299 cells, hESCs grow very poorly as single cells and require close contact with neighboring cells.

Inconsistencies with both hydrogels mentioned (such as slide to slide variation in cell attachment/proliferation) may signify one of two issues: 1) hESCs are not supported by these polymer hydrogels as substrates, 2) varying surface morphologies due to dehydration procedure creates different microenvironments, and thereby differentially supports hESC culture. However, partially successful cultures of hESCs on Polymer #8 and #12 hydrogels for multiple passages suggest that these polymers do have potential for supporting hESC attachment and proliferation. The results indicate that differences in morphology may account for the variations in cell attachment.

Controlling the morphology of surfaces that cells reside on is important for future work on polymer substrates. There are a number of distinct possibilities for long-term analysis of polymers that support hESC culture on more traditional culture formats. Using polymers #8, #12 and #24, it is possible to use solvent casting to deposit them onto a tissue culture dish. This simple method involves dissolving the polymer in a solvent of interest, and using the airflow in a tissue culture hood to evaporate the solvent, leaving the polymer deposited on the surface of the dish. The advantage of testing hESCs in this format is that the cells attach to coated tissue culture plates. The mechanical and surface properties of these plates do not vary from

one dish to the next. HESCs can be supported by the coated tissue culture plates, just as they are supported by dishes coated with Matrigel. Thus, this method would eliminate the variable of surface morphology while analyzing polymers as substrates. However, solvent casting leaves a heterogeneous deposition of polymer on the surface of the plate. This could lead to patches of cell adherence onto tissue culture dishes. Although this method would be successful at analyzing cell adherence on polymer substrates, it would make it difficult for quantitative cellular analysis. Another possibility is to spin coat the polymers onto the dishes, thereby ensuring a homogeneous layer of polymer on the tissue culture dish. Since this requires a spin coater, this method is more expensive, but would allow for characterization of cell properties such as rates of proliferation.

RNA INTERFERENCE

Introduction

RNA interference (RNAi) refers to the "conserved biological response to double-stranded RNA" that is characterized by post-transcriptional gene-specific silencing [36]. RNAi was first discovered in 1998 through experimentation with double-stranded RNA (dsRNA) in the organism *Caenorhabditis elegans* [37]. Fire, *et al*. observed gene-specific silencing following introduction of specific dsRNA templates by an unknown mechanism. Further research established that RNAi was "evolutionarily conserved" (occurring across various species) and elucidated the pathways of gene-specific silencing by dsRNA [38, 39].

Gene-specific silencing occurs through the effect of the ribonuclease (RNase) enzyme Dicer on double stranded RNA. Dicer cleaves the dsRNA into double-stranded small interfering RNAs (siRNAs) of approximate length of 23 nucleotides [40]. These siRNAs then can either act through the RNA-induced silencing complex (RISC) to degrade complementary mRNA sequences, or possibly through the RNA-induced transcriptional silencing (RITS) complex to repress transcription and modify DNA and histone methylation [40].

The goal of this study was to evaluate the utility of the arrayed cellular microenvironment technology platform for performing RNAi screens. Previously, scientists have constructed libraries of siRNA molecules to dissect biological processes in a genome wide fashion. Traditionally these RNAi screens were performed by transfection of the siRNA molecules into cells plated in 96 or 384 well plates and assaying a biological process of interest. This high throughput method of

characterizing protein loss-of-function has proved to be an effective method to discover functions of unknown genes and further understanding of cell biology [41-43].

We would like to utilize our arrayed cellular microenvironment technology to perform such a RNAi screen. A major advantage of doing so would be that the screen could be substantially reduced in size. For example, for a library consisting of 10,000 individual siRNA molecules, a total of over one hundred 96-well plates would be required. In contrast, with the cellular microarrays this type of screen could be performed with as few as 10 slides, each carrying 1,000 spots.

Unfortunately, naked siRNA molecules are not readily taken up by cells [44]. To circumvent this problem and deliver siRNA molecules into cells growing on the cellular microarrays, we collaborated with researchers with expertise in siRNA delivery. Dr. Steven Dowdy's lab at UCSD has developed a peptide transduction domain – double stranded RNA binding domain (PTD-dRBD) molecule that binds siRNA duplex load. The PTD domain of this protein promotes uptake of the protein-RNAi complex into the cell through a process of "cell drinking" or macropinocytosis [45]. Peptide transduction domains were discovered after experimentation with HIV-1 TAT protein [46]. Subsequent analysis elucidated the specific peptide sequences on this protein that allowed for it to defy the size limitations of molecules crossing the membrane barrier [47]. After cellular uptake, the dsRNA separates from the PTD-dRBD complex and acts through the RNA interference pathways [45]. Using the PTD-dRBD-siRNA complex, we would like to test whether we can deliver siRNA molecules into cells. As proof-of-principle, we attempted to knock-down expression of

a green fluorescent protein (GFP) with this PTD-mediated siRNA delivery system. With statistical measurement techniques already in place, the capability of performing siRNA screens has the potential to be a significant addition to this multifaceted technology.

Results

Before moving forward with siRNA studies on the array platform, we needed to develop an assay to test the functionality of the PTD-dRBD-siRNA complex (hereafter referred to as the PTD-siRNA complex) in a larger, more common format. First, we created a GFP assay on a plate reader (Perkin Elmer Envision 2103) through experimentation with HEK-293 and HEK-293 GFP cells. In order to characterize the sensitivity of the plate reader in reading GFP signal, we performed an experiment where we mixed HEK-293 and HEK-293 GFP cells in various ratios in a 96 well plate with 50,000 cells total per well. We varied the amount of each cell type as illustrated in Figure 16a. Given this experimental setup, we were able to determine whether the plate reader was capable of determining 10% differences in GFP signal. As seen in Figure 16b, the fluorescent signal from the plate reader increased linearly with 10% increases of HEK-293 GFP cells (with R^2=0.983), thereby demonstrating the capability of the instrument in detecting slight variations in GFP signal.

Once we established this GFP assay, we began experimenting with the corresponding PTD-(GFP) siRNA. On the same 96-well format, we tested our PTD-siRNA complex on HEK-293 GFP cells (n=3 wells) and compared the GFP signal to untreated control samples (n=9 wells) at 24 and 48 hours after treatment of siRNA (Fig. 17a). The GFP signal is slightly diminished in the siRNA treated samples. Yet

without further analysis we cannot determine whether this loss of GFP expression is due to cell loss caused by the siRNA treatment protocol, or actual siRNA inhibition of GFP expression. Since it was not our goal to optimize the siRNA inhibition on our HEK-293 GFP cell line but rather to prove the principle of siRNA screening capability on the array format, we tested the efficacy of the PTD-siRNA complex to knockdown GFP expression in cells that were previously tested in this assay. The Dowdy lab provided us with a cell line, H1299-CMV-GFP, for siRNA studies.

Using these cells we detected a significant reduction in GFP expression in cells treated with the PTD-siRNA complex compared to untreated cells (Fig. 17a). The confocal microscope images show a similar effect; the GFP expression in the siRNA treated cells is greatly diminished in comparison to the untreated cells (Fig 17b). Knockdown of GFP signal in GFP H1299 cells treated with siRNA is nearly complete. To ensure that this reduction in GFP signal was due to a RNAi effect rather than a decrease in cell number, we quantified total protein using a Coommassie stain 48 hours after siRNA treatment (Fig. 19a). We observed only a slight difference in total protein, thus demonstrating that the reduction of GFP signal is due to a RNAi mechanism. This is displayed in Figure 19b through normalizing GFP signal by total protein signal. To further characterize this difference, we immuno-blotted protein samples from siRNA treated and untreated cells with antibodies to both GFP and β-tubulin (Fig. 19c). β-tubulin serves as a loading control and its levels should be unaffected by the siRNA treatment. As expected, the GFP band intensity on the Western blot was significantly reduced relative to the β-tubulin control band in siRNA

treated cells. This result demonstrates that the PTD-siRNA complex was successful at crossing the cell membrane and inhibiting GFP expression.

Once we established that siRNA inhibition of GFP was occurring, we spotted the PTD-siRNA using our previously designed array format. The PTD-siRNA complex was spotted along with collagen I, an extracellular matrix protein that allows cells to adhere to microarray spots [3], thereby theoretically allowing for the PTD-siRNA complex to be taken in by the cells. We spotted using two different methods: 1) the PTD-siRNA mixed with collagen I, and 2) the PTD-siRNA spotted on top of (labeled "after" in Fig. 20a-b) collagen I.

In both methods of spotting, the effects of the siRNA on the array format seemed to be negligible (Fig. 20a-c). A small knockdown of GFP expression was observed when spotting PTD-siRNA on top of the Collagen I; however, with a p value of 0.31, this decrease in signal was not statistically significant. The GFP signal remains consistently high on both siRNA treated and untreated control cells. This can be due to three major causes; 1) the PTD-siRNA complex was not retained in the spots, 2) the activity of the PTD-siRNA was lost during the printing process, or 3) not enough siRNA was taken up by the cells, causing a small knockdown of signal that could not be measured.

In order to confirm that the PTD-siRNA complex was retained in the spots, we stained two arrays with an anti-HA antibody (Covance). The PTD-dRBD carries a HA tag and consequently can be detected by immuno-blotting with anti-HA antibody. One array we stained and observed directly, in order to determine if the PTD-siRNA was successfully deposited. We placed the second array in PBS for 24 hours to determine

of the PTD-siRNA diffused out of the spots. In both cases, we observed that the PTD-siRNA was still retained in the spots (data not shown). Thus, we determined that the main cause for lack of siRNA activity was due to either loss of activity of the PTD-siRNA complex or lack of enough siRNA uptake to cause RNA interference.

Discussion

In this section we have demonstrated the capability of the PTD-dRBD-siRNA complex to traverse the cell membrane and inhibit GFP expression. However, on the arrays we were unable to show statistically significant siRNA-induced knockdown of gene expression. This lack of knockdown can be due to various considerations (e.g. siRNA degradation, concentration), and requires further analysis. Future experimentation would involve spotting increased concentrations of the PTD-siRNA complex, and cooling and accelerating the array printing process to reduce potential siRNA degradation. In our experiments, we spotted proteins and siRNA on day one, stored the slides at 4 degrees overnight, and seeded with cells the following day. Alternatively, to reduce chances of loss of PTD-siRNA complex activity due to siRNA degradation, it may be beneficial to expedite the process and seed with cells immediately after spotting.

Although we were not able to demonstrate the capability of a siRNA screen on our array technology, these preliminary experiments demonstrate the success of the PTD-dRBD-siRNA uptake into cells and hold promise for future siRNA screening adaptations. Further research in the specific areas noted above could make it possible to successfully screen various siRNAs on this microarray platform.

CONCLUSION

Throughout this paper, we have explored the diverse applications of the arrayed cellular microenvironment technology. From discovery of substrates for human embryonic stem cell (hESC) culture to potential methods for high throughput siRNA screens, we have demonstrated the versatility of this technology and displayed how it can contribute to further understanding of the cellular microenvironment.

In Brafman *et al.* [3], we used the technology to discover an optimal combination (Collagen 1, Collagen 4, Fibronectin, Laminin, or C1+C4+Fn+Ln) of extracellular matrix proteins (ECMPs) for hESC culture. In this paper, this defined matrix was further characterized using quantitative PCR analysis. We demonstrated that hESCs grown on C1+C4+Fn+Ln maintain pluripotency (as measured by Oct4 and Nanog expression levels) at equal or greater levels than Matrigel. We established that a reduced concentration of these factors (from 10 $\mu g/cm^2$ to 5 $\mu g/cm^2$) was also able to support maintenance of pluripotency in hESCs. We verified that this defined matrix maintains pluripotency in hESCs by creating embryoid bodies and displaying increased gene expression of lineage-specific factors, indicating differentiation. This work demonstrates the potential of the defined matrix of C1+C4+Fn+Ln as a substrate for hESC culture.

Through our high throughput polymer screens, we were able to discover a set of polymers that support adherence and proliferation of hESCs. Using these identified polymers (Polymer #8 and #12), we experimented with traditional cell culture formats to characterize long-term culture potential on these polymer substrates. Although

culture was possible through four passages, inconsistent results necessitate future research using different polymer coating techniques on tissue culture plates.

Lastly, we investigated a novel high throughput method for siRNA delivery using peptide transduction domains fused to a double stranded RNA binding domain (PTD-dRBD). These molecules facilitate uptake into cells through the PTD and bind a siRNA duplex using the dRBD. We displayed the capability of these PTD-dRBD-siRNA complexes to traverse the cell membrane and inhibit specific gene of interest (in our case, Green Fluorescent Protein). However, we were unable to demonstrate significant knockdown of GFP signal on the array platform. Future study would involve increasing concentrations of spotted PTD-dRBD-siRNA complexes or reducing the time before seeding with cells to avoid siRNA degradation.

The arrayed cellular microenvironment technology is not limited to the applications which we have described. This technology can be implemented toward investigations into conditions that would allow for expansion of difficult-to-culture primary cell lines, combinatorial signaling of proteins, glycans and cytokines, and even disease modeling. This adaptable array platform is a valuable tool for high throughput analysis of cellular conditions, and will continue to simplify the process of discovery-based research in cell biology.

MATERIALS AND METHODS

Cell Culture

For the various cell lines used, cell medium consisted of:

1) HEK-293, H1299, and MEF: 1X high glucose DMEM (Invitrogen), 10% Fetal Bovine Serum (Invitrogen), 1% L-glutamine penicillin/streptomycin (Invitrogen).
2) H9/WA09: 1X DMEM-F12 (Invitrogen), 20% Knockout Serum Replacement (Invitrogen), 1% non-essential amino acids (Invitrogen), 0.5% glutamine (Invitrogen), 120μM 2-mercaptoethanol (Sigma).
3) Hues 1 and Hues 9: 1X Knockout DMEM (Invitrogen), 10% Knockout Serum Replacement, 10% Human Plasmanate (Talecris Biotherapeutics), 1% non-essential amino acids, 1% penicillin/streptomycin, 1% Gluta-MAX (Invitrogen), 55 μM 2-mercaptoethanol.

MEF-Conditioned Media is made by culturing MEFs in presence of hESC medium for 24 hours, and StemPro medium is made up of StemPro supplement in 1X DMEM-F12, 2% BSA (Millipore), and 55 μM 2-mercaptoethanol. All percentages listed are by volume.

Hues 1 and Hues 9 cells were passaged through enzymatic dissociation using Accutase (Millipore) for 4-5 minutes at 37°C and centrifuged at 200 x g after addition of cell medium. H9 cells were passaged using Dispase (Invitrogen) for 5-6 minutes at 37°C, rinsed with medium 3 times, and dissociated with a cell scraper. Furthermore, colonies were fragmented by repeated pipetting before transfer to new plate. Basic

Fibroblast Growth Factor (bFGF, Invitrogen) was added to all stem cell cultures at 30 ng/ml.

To seed the arrays with cells, HEK-293s, H1299s, and MEFS (2.5 x 10^5/slide) were all passaged straight onto the glass slides. In order to decrease contamination by MEF feeder layer cells, hESCs (Hues 1m Hues 9 and H9) were grown on Matrigel (BD) for 2 passages using MEF-Conditioned Media with the additive bFGF. The cells were then passaged onto the arrays using Accutase as described above with a cell concentration of 5 x 10^5 per slide. The hESCs were fed (and supplemented with bFGF) daily.

For long-term culture of hESCs on the defined conditions established by Dave Brafman [3], cells were first grown on Matrigel for 2 passages, as described above. Extracellular matrix proteins (ECMPs) were coated onto tissue culture dishes at 10 μg/cm^2, and cells were passaged onto these dishes at concentration of 5 x 10^4 cells/ml. The cells were fed daily with medium (either MEF-Conditioned Media or StemPro) and bFGF.

Immunocytochemistry and Imaging

Cells on the arrays were permeabilized with 0.2% Triton X-100 (v/v) and blocked with 1% (w/v) BSA and 3% (w/v) milk for 30 minutes. Cells were stained for DNA with Hoechst 3342 (2 μg/ml; Invitrogen) for 5 minutes, and primary antibodies rabbit-anti Oct3/4a or rabbit-anti-Nanog (Santa Cruz) at 1:200 dilution in 1% BSA overnight. After TBS washes, cells were treated with goat-anti rabbit Alexa 647 secondary at 1:400 for 1 hour at 37°C. Cells were fixed in 4% PFA for 5 minutes at 4°C, and subsequently 10 minutes at room temperature. Imaging of slides was done

using a automated confocal microscope (Olympus Fluoview 100 with motorized stage). Each subarray was imaged individually, and images were analyzed using GenePix (MDS Analytical Technologies).

Embryoid Body Formation

A day before EB formation, cells were treated with 5 μM ROCK inhibitor. Cells were then trypsinized and passaged into an untreated v-shaped 96 well plate at a concentration of 5 x 10^3 cells/well. The plate was centrifuged at 950 x g and incubated overnight. Cells from the 96-well plate were then pipetted using a P1000 into an ultra-low binding 6-well plate at concentration of approximately 60 EBs per well. EBs remained in 6-well plates for 1 week, and were fed every 2-3 days by gentle removal and addition of media using serological pipette. Finally, EBs were plated onto a Matrigel coated 6-well dish and grown for 2 weeks.

Quantitative RT-PCR

RNA was isolated from cells using TRIzol (Invitrogen), and treated with DNase I (Invitrogen) to remove traces of DNA. Reverse transcription was performing by means of qScript cDNA Supermix (Quanta Biosciences). Quantitative PCR was carried out using TaqMan probes (Applied Biosystems) and TaqMan Fast Universal PCR Master Mix (Applied Biosystems) on a 7900HT Real Time PCR machine (Applied Biosystems). Probes used were GAPDH: Hs99999905_m1 as endogenous control, OCT4: Hs00742896_s1, and NANOG: Hs02387400_g1. Alternatively, TaqMan Low Density Arrays are preloaded with probes, thus only needing to be loaded with sample and Fast Universal PCR Master Mix. Clustering analysis of results

was done using Gene Cluster (Eisen) and heat maps were generated in Treeview (Eisen).

Array Fabrication/Polymer pad formation

Arrays are printed onto acrylamide hydrogel pads on silanized glass slides (75mm x 25mm x 1mm). Hydrogel pads of various polymers (i.e. Polymer #8 and #12) are also formed on silanized slides. Slides were cleaned through washes in 100% acetone, 100% methanol, and multiple rinses of Millipore H_2O (MQH_2O), followed by etching in 0.05M NaOH overnight. After repeated rinsing with MQH_2O, slides were air-dried and baked in a vacuum oven at 65°C and 20psi for 1 hour. The glass slides were then silanized overnight using 2% 3-(trimethoxysilyl)propyl methacrylate in toluene, and once again baked in a vacuum oven at 65°C and 20psi for 1 hour.

To form hydrogel pads, an appropriate concentration of a monomer (acrylamide, #8, or #12) is mixed with the crosslinker bis-acrylamide (also at specific concentration) in either PBS or H_20. For array slides, 10% (w/v) acrylamide is mixed with 0.55% (w/v) bis-acrylamide in MQH_20. For polymer hydrogels, monomer #12 is mixed with bis-acrylamide at the same concentration in PBS, while in Polymer #8 gels 1% bis-acrylamide is used in PBS. A photoinitiator, Irgacure 2959 (Ciba Specialty Chemicals), is diluted in methanol at 20% weight per volume, and mixed 1:10 with the previous solutions. Thus, a stock solution, made up of 10% monomer, varying percentages of crosslinker (0.55% or 1%), and 2% photoinitiator, is prepared. Next, 100 µl of this solution is pipetted onto a silanized glass slide, covered with a coverslip (Bellco Glass), and exposed to 1.5 mW/cm2 365-nm ultraviolet A light. For acrylamide pads to be used for arrays, UV exposure is 7 minutes, while for Polymer

#8 and #12 hydrogels exposure is 30 minutes. The Polymer #8 and #12 gels formed are treated in one of 2 ways. 1) They are soaked in PBS for 10 minutes; the coverslip is removed, and continually swelled for 24 hours in PBS with antibiotics (Penicillin/Streptomycin). Subsequently, the slides are soaked in 70% ethanol for 3 hours, followed by 8 washes in PBS + Penicillin/Streptomycin over 2 days, at which point they are ready to be seeded with cells. 2) The coverslip is removed after 10 minutes of soaking in MQH_2O, followed by further soaking for 48 hours. The slides are then dehydrated through the use of a hot plate at 40°C for 10 minutes, which completes preparation for printing (this is the method used for acrylamide gel pads also).

For printing, extracellular matrix proteins (ECMPs) of interest are diluted in printing buffer made up of 200 mM acetate, 10 mM EDTA, 0.5% (v/v) triton X-100, and 40% (v/v) glycerol in MQH_2O. For ECMPs, acetic acid was added to adjust the pH to 4.9. Polymers were dissolved in DMSO. ECMPs were spotted at 250 μg/ml, while polymers were spotted at a concentration of 4 mg/ml.

Printing was performed on the glass slides with acrylamide pads using a SpotArray 24 (Perkin Elmer) at 65% humidity. One a single slide, spots were done in 16 10 x 10 subarrays, with spots being 150 μm in diameter and 450 μm apart from each other. Spots were done in five replicates. After printing is completed and before the array slides are seeded with cells, slides are rinsed in PBS and placed under UV radiation for 10 minutes in the biosafety hood.

PTD-dRBD-siRNA Treatment

Cells were counted and passaged into a 96-well plate at a concentration gradient of 5,000 to 30,000 cells per well and incubated overnight. Wells are then selected by visual approximation of 80% confluency. Then, the PTD-dRBD-siRNA complex is prepared: for each well to be treated, 2.4µl of PBS-10% glycerol, 4.8µl of 50µM PTD-dRBD protein, and 4.8µl of 5µM siRNA are mixed gently by pipetting and incubated on ice for 15 minutes. Subsequently, 48ul of serum-free DMEM is added to the mixture of PTD-dRBD-siRNA, and mixed by pipetting. This solution is 4% (v/v) PBS-glycerol, 8% (v/v) 50 µM PTD-dRBD, and 8% (v/v) 5µM siRNA in DMEM. Cells are then prepared by a PBS rinse, following by addition of this 60ul solution of DMEM/PTD-dRBD-siRNA per each well. Cells are incubated for 6 hours in this solution at 37°C. After 6 hours, cells are rinsed twice with medium (with serum) and monitored at the 24 and 48 hour time points.

Plate Reader GFP assays

To quantify and analyze GFP signal, we used an Envision multilabel plate reader (Perkin Elmer). The excitation filter used was of wavelength 486 nm, and the emission filter was of wavelength 530 nm.

APPENDIX

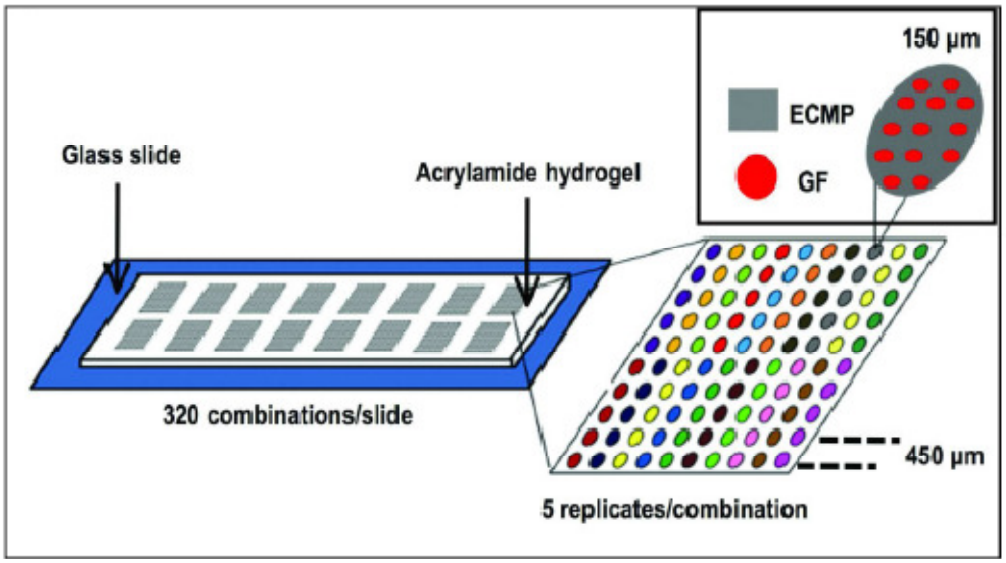

Figure 1. Design of arrayed cellular microenvironments. Arrays of ECMPS (or polymers) are spotted in 16 subarrays containing 100 spots in a 10 x 10 arrangement. 5 replicates are printed of each individual combination. Reproduced with permission from Brafman, *et al* [3].

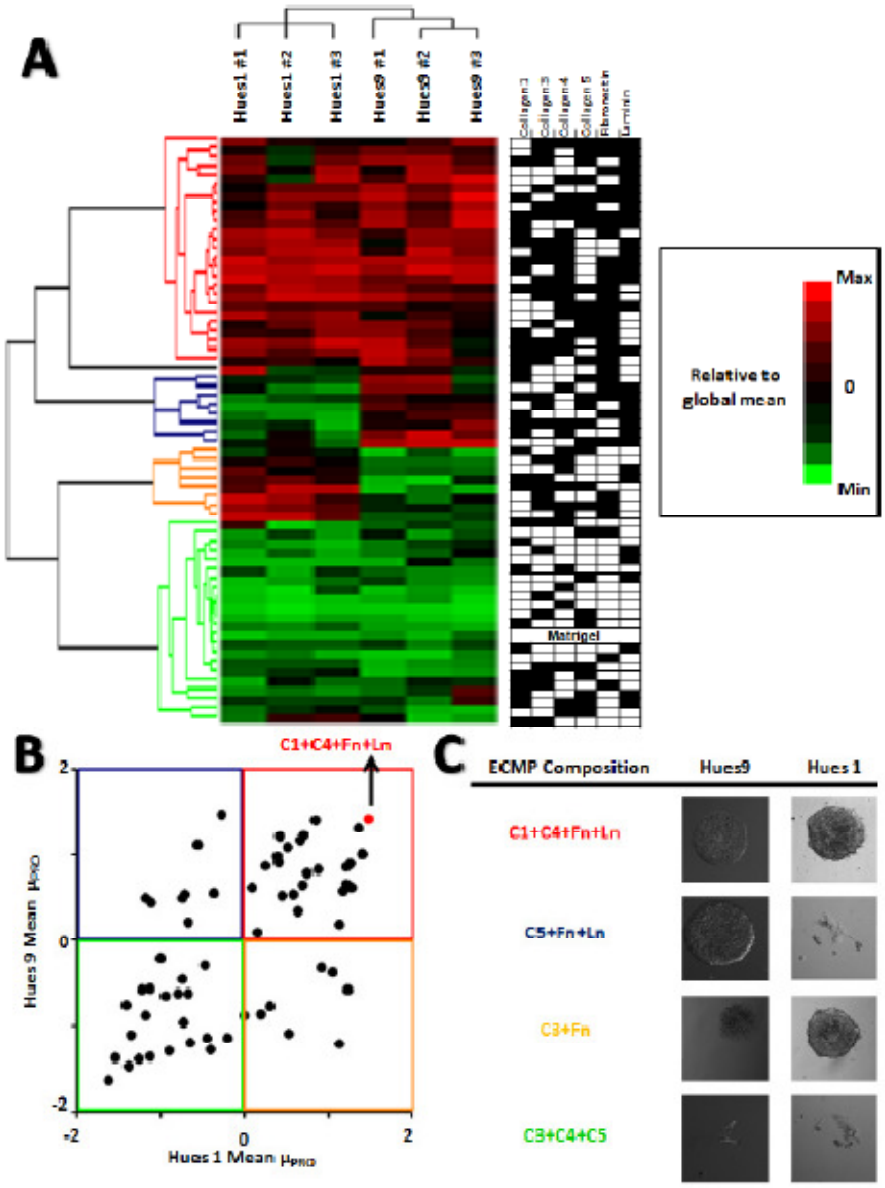

Figure 2. Effects of ECMP combinations on proliferation in hESCs. **A)** Two-way Clustering of mean proliferation (rows) across experiments (columns) using 2 cell lines (Hues **1** and Hues 9) into a heat map. ECMPs present in each row are indicated by darkened boxes**.** The red cluster indicates high proliferation in both Hues **1** and Hues 9. **B)** Z-scores of mean proliferation values divided into 4 regions seen in heat map. C1+C4+Fn+Ln has high proliferative effect in both cell lines. **C)** Representative phase contrast images of the 4 clusters. Reproduced with permission from Brafman, *et al.* [3].

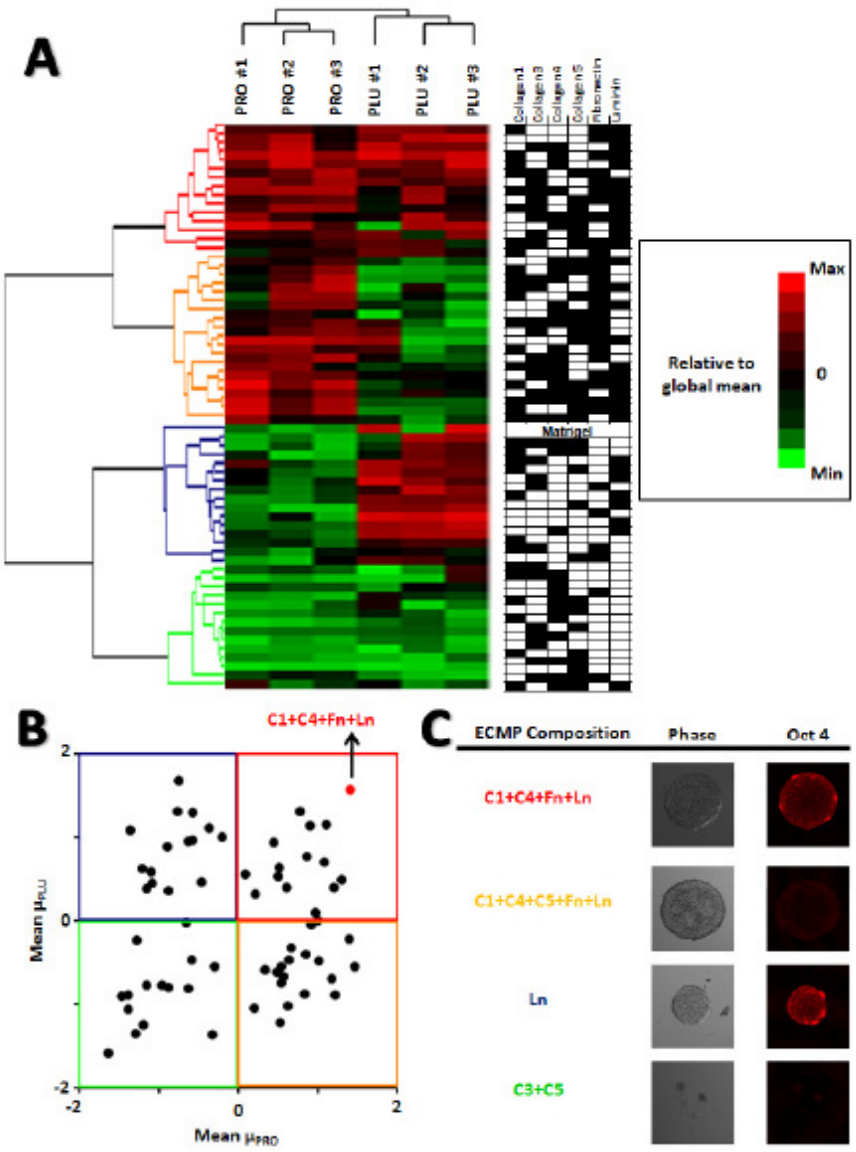

Figure 3. Effects of ECMP combinations on pluripotency and proliferation in hESCs. **A)** Two –way clustering of mean proliferation and pluripotency (rows) across experiments (columns). ECMPs present in each row are indicated by darkened boxes. The red cluster indicates high proliferation and pluripotency. **B)** Z-scores of mean proliferation values plotted against Z-scores of mean pluripotency ratios. C1+C4+Fn+Ln has both a high proliferative and pluripotency indices. **C)** Representative phase contrast and Oct-4 stained images of the 4 clusters. Reproduced with permission from Brafman, *et al.* [3].

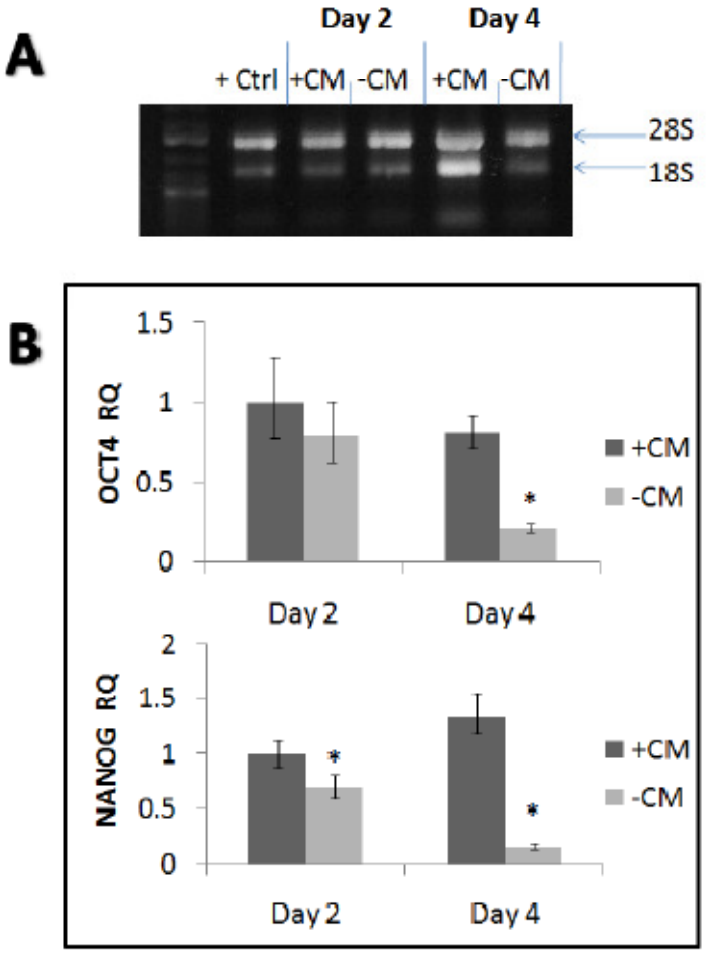

Figure 4. RNA isolation and quantitative PCR assay development. **A)** Electrophoresis of RNA from cells grown in presence of conditioned medium (+CM) or without it (-CM). **B)** Quantitative PCR (qPCR) of Day 2 and Day 4 samples seen in A) relative to Day 2+CM. Samples grown without CM (-CM) display a >5 fold drop in Oct-4 and Nanog expression by Day 4.

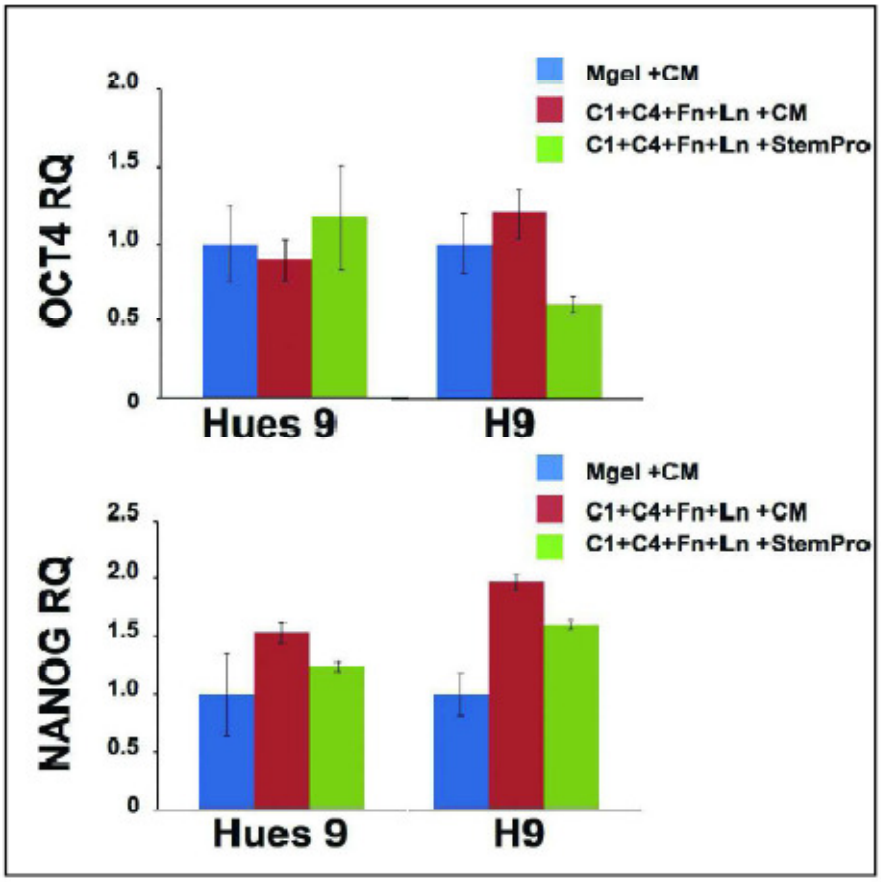

Figure 5. Expression on defined matrix at passage 10. Mean Oct-4 and Nanog gene expression at passage 10 on C1+C4+Fn+Ln in StemPro or conditioned medium (CM) in Hues 9 and H9 cell lines. The fold change is respective to Matrigel +CM. Reproduced with permission from Brafman, *et al* [3].

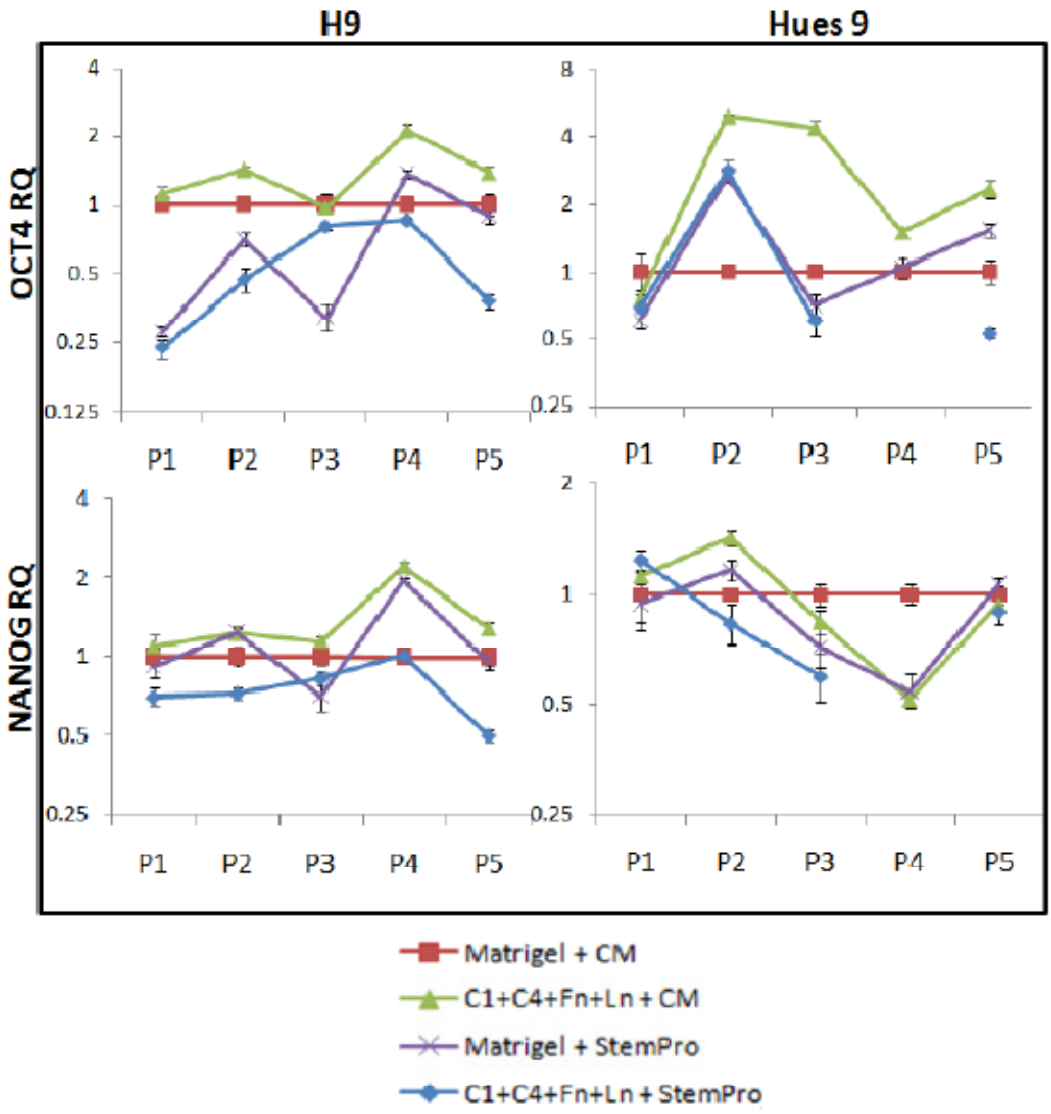

Figure 6. Maintenance of pluripotency on the defined matrix. Oct-4 and Nanog expression on C1+C4+Fn+Ln in conditioned media (CM) and StemPro relative to Matrigel + CM across 5 passages in H9 and Hues 9 cell lines. Oct-4 and Nanog levels in defined matrix + CM (green) are equal to or above Matrigel+CM across all passages except for Hues 9 Nanog passage 4, which is explained in Fig. 10.

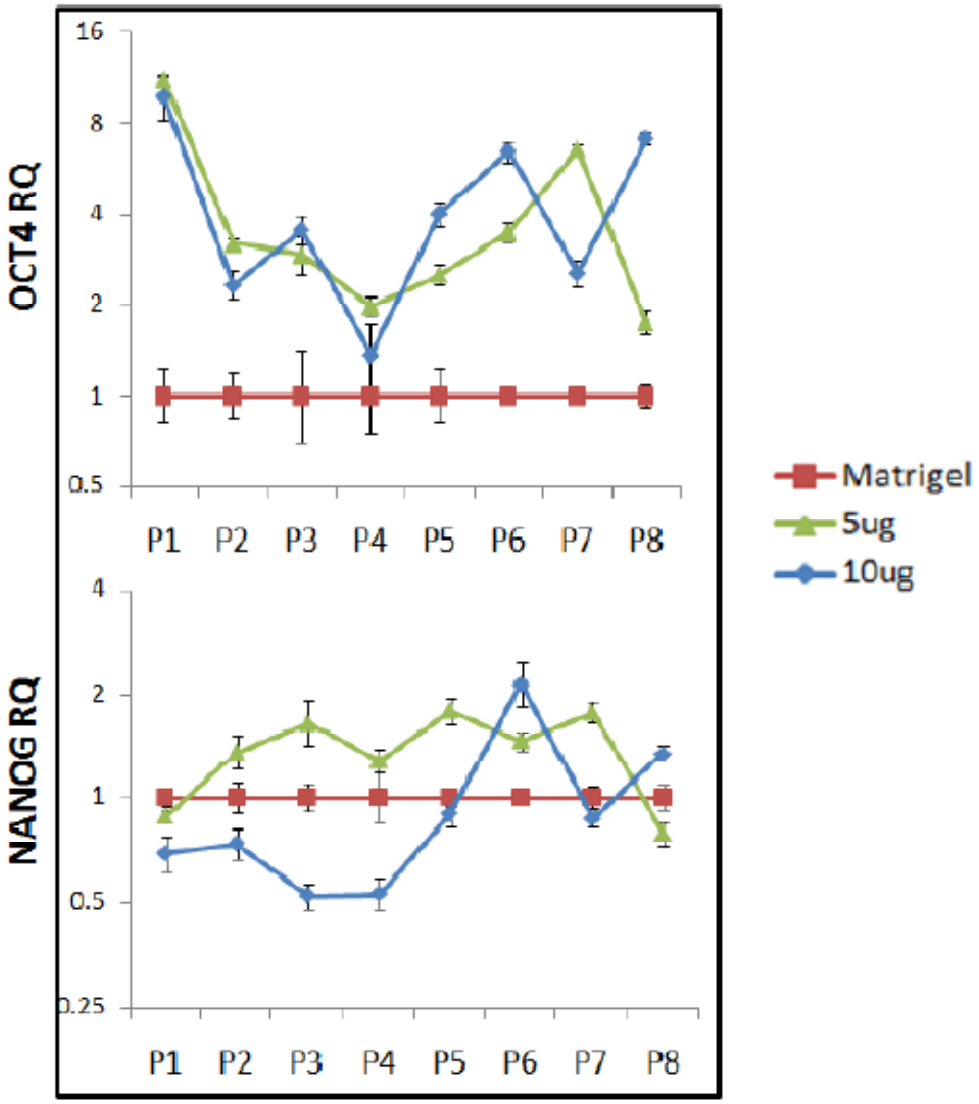

Figure 7. Effects of reduced ECMP concentration on maintenance of pluripotency. Oct-4 and Nanog relative expression to Matrigel across 8 passages on Hues 1 cell line. Concentrations listed are per cm^2 of tissue culture dish (e.g. 10 $\mu g/cm^2$ and 5$\mu g/cm^2$). Oct-4 and Nanog expression in 5 $\mu g/cm^2$ ECMPs appears greater than in Matrigel.

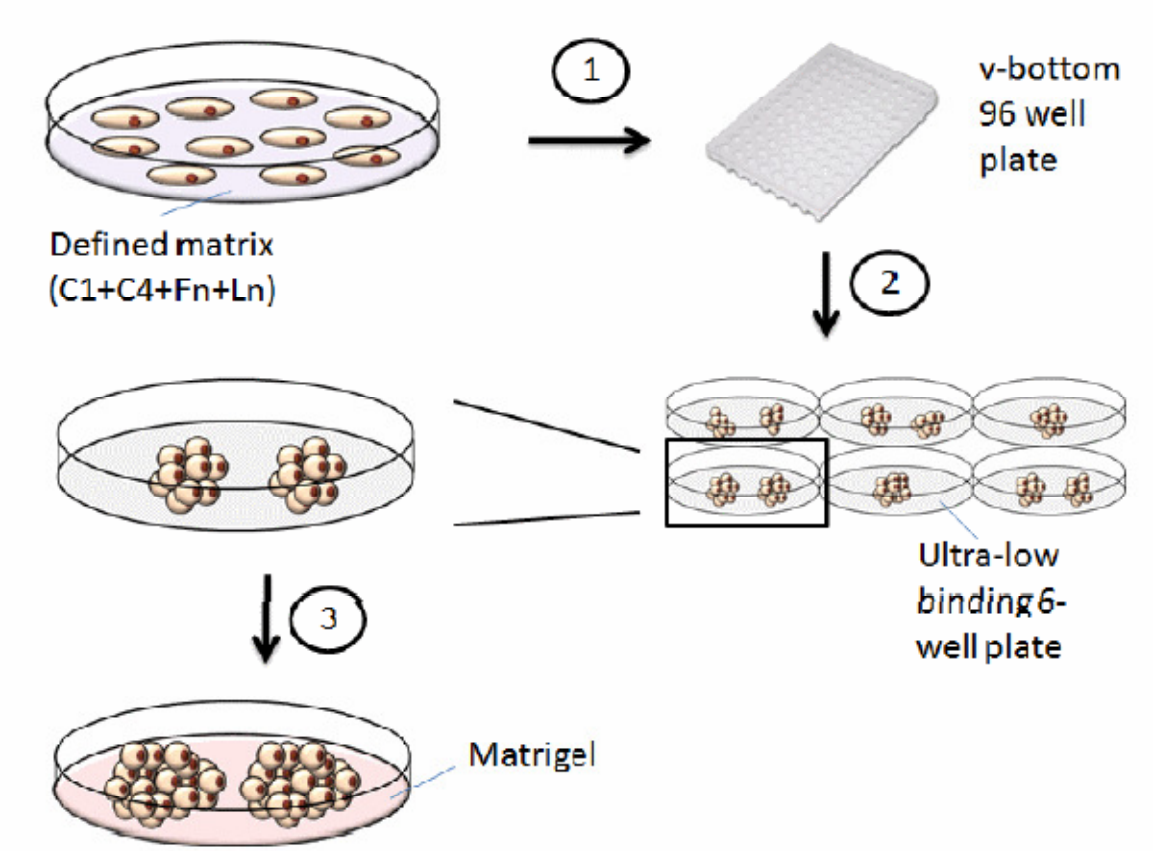

Figure 8. Embryoid body formation from hESCs grown on defined matrix. **1)** Cells are treated with Rock inhibitor, passaged into v-bottom 96 well plate at 5,000 cells/well and centrifuged. **2)** After overnight incubation, cells are pipetted into ultra-low binding 6-well plates. **3)** After 1 week, EBs are transferred to Matrigel coated 6-well dishes and grown for 2 weeks.

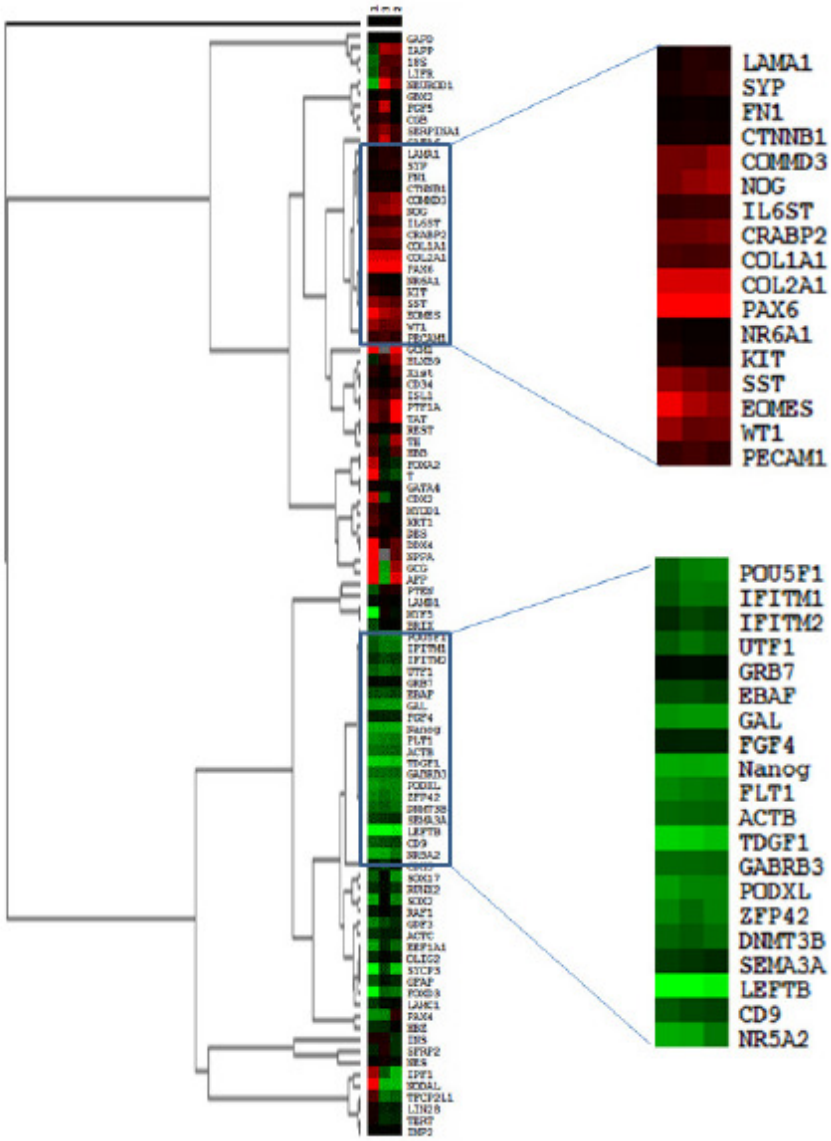

Figure 9. Gene expression in Embryoid Bodies. Genes upregulated (red) and downregulated (green) in Embryoid bodies grown on the defined matrix relative to undifferentiated hESCs. Upregulated genes seen in cluster include Endoderm (LAMA1, FN1, SST), Ectoderm (SYP, PAX6, PECAM), Mesoderm (COL1A1, COL2A1, WT1), and Trophoblast (EOMES) layers, indicative of differentiation. Yet, stemness genes are also upregulated (COMMD3, NOG, IL6ST, CRAB, NR6A1, KIT), suggesting heterogeneity of EBs. The downregulated cluster of genes are strongly associated with stem cell state: both pluripotency (POU5F1 [Oct-4], NANOG, TDGF1, GABRB3, DNMT3B) and stemness (IFITM1, IFITM2, UTF1, GRB7, EBAF, GAL, FGF4, PODXL, ZFP42, SEMA3A, LEFTB, CD9, NR5A2) markers are seen.

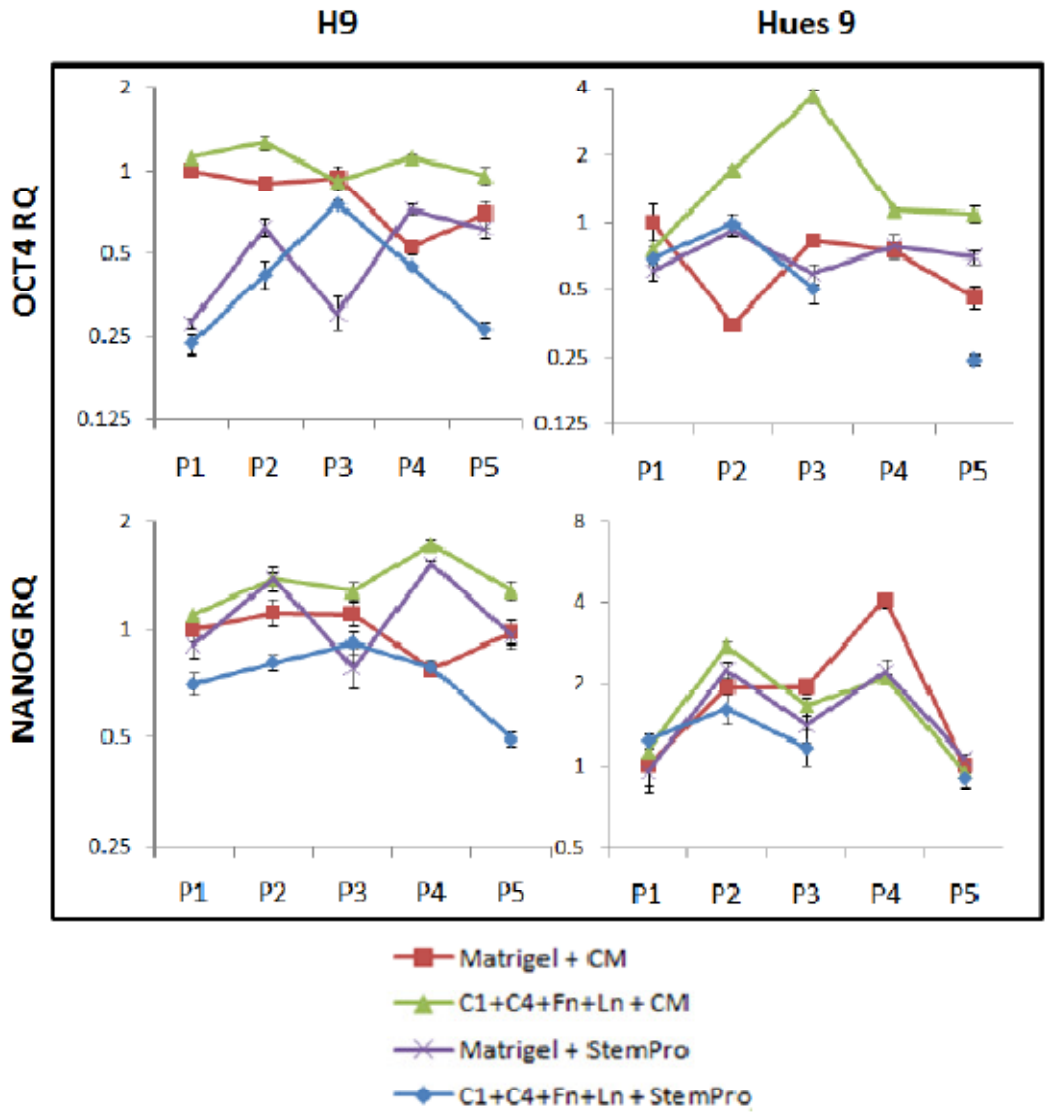

Figure 10. Maintenance of pluripotency on the defined matrix relative to Matrigel Passage 1. This figure is a reproduction of Figure 6 using Matrigel P1 as the calibrator (instead of each Matrigel passage), depicting the fluctuations seen in Matrigel Oct-4 and Nanog expression. Nanog expression in Hues 9 Matrigel P4 is an outlier which influences the results seen in Figure 6.

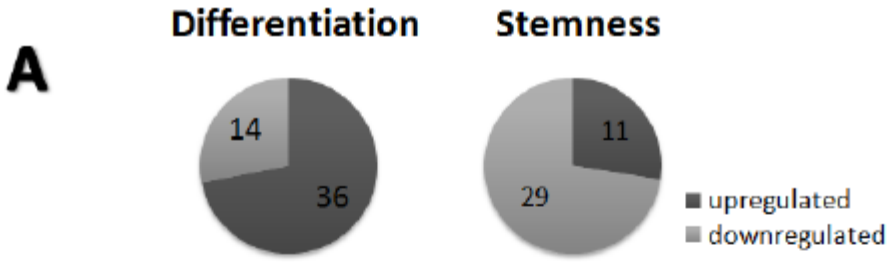

B

	Markers							
	Pluripotent	Stemness	Trophoblast	Ectoderm	Mesoderm	Endoderm	Germ	**Total**
Upregulated	0	11	5	9	8	13	1	47
Total	7	33	5	13	12	18	2	90
% Upregulated	***0***	***33***	***100***	***69***	***67***	***72***	***50***	***52***

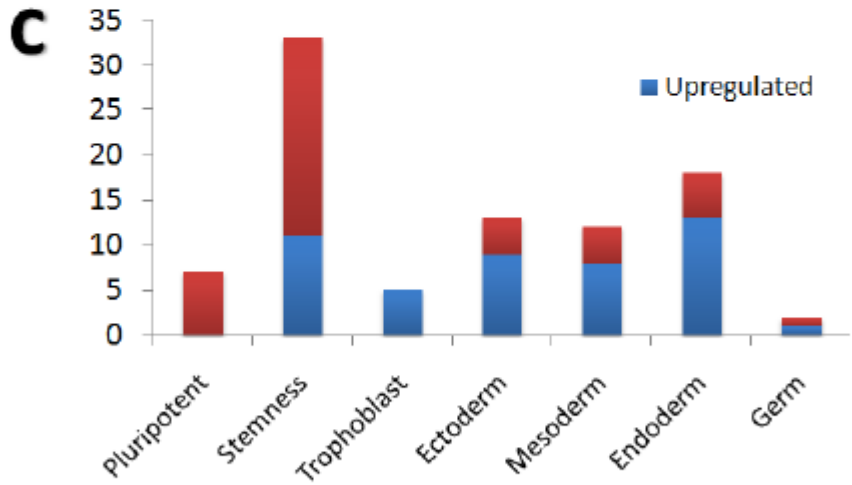

Figure 11. Average gene expression in Embryoid bodies. **A)** Of 96 genes total on TaqMan pluripotency arrays, 50 are differentiation specific and 40 are related to stem cell state. 72% (36/50) of differentiation genes are upregulated while 27.5% (11/40) of stem cell associated genes are upregulated. **B-C)** Percentage of upregulated markers seen in each category (pluripotency, stemness, trophoblast, ectoderm, mesoderm, endoderm and germ).

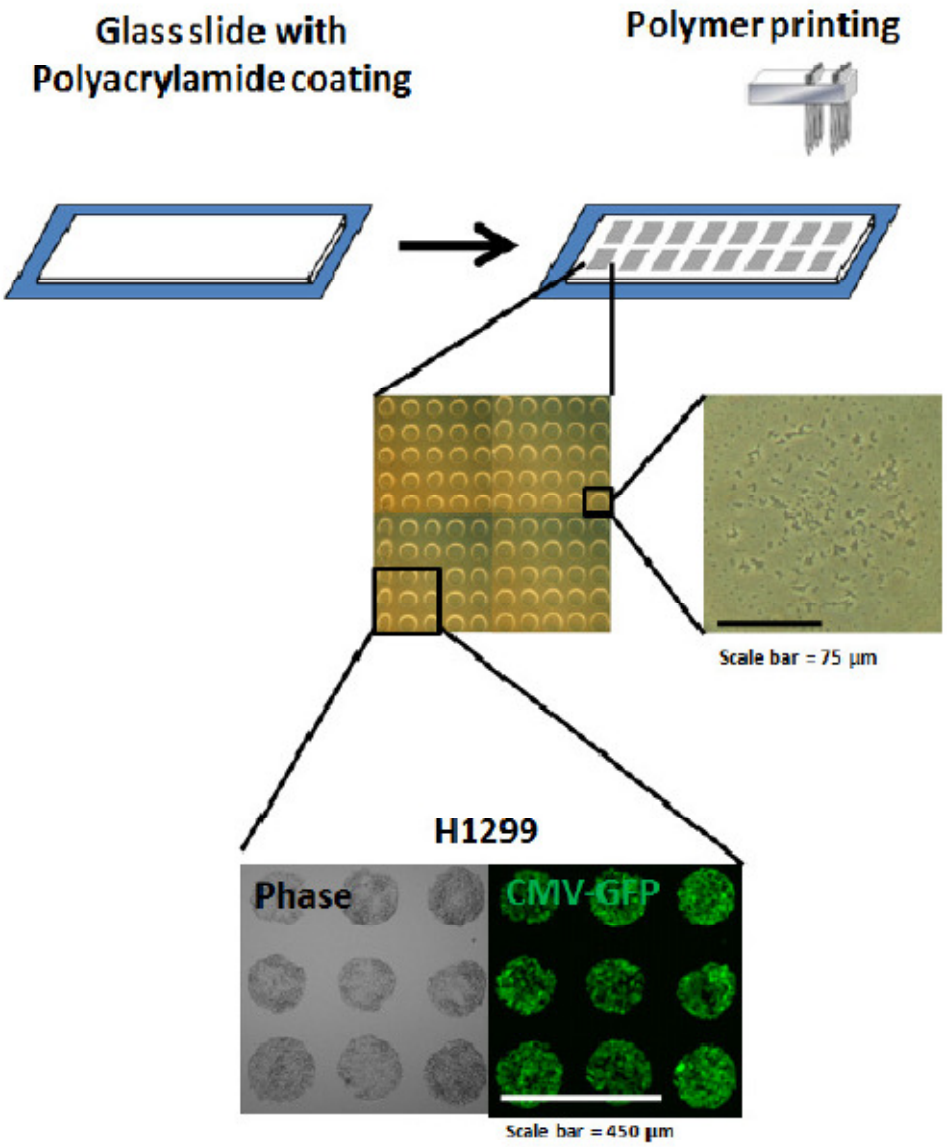

Figure 12. Polymer printing procedure. Glass slides were silanized and coated with an acrylamide gel pad. Polymers were than printed using a microarray spotter. Cells were then seeded globally, and attach selectively to polymer spots.

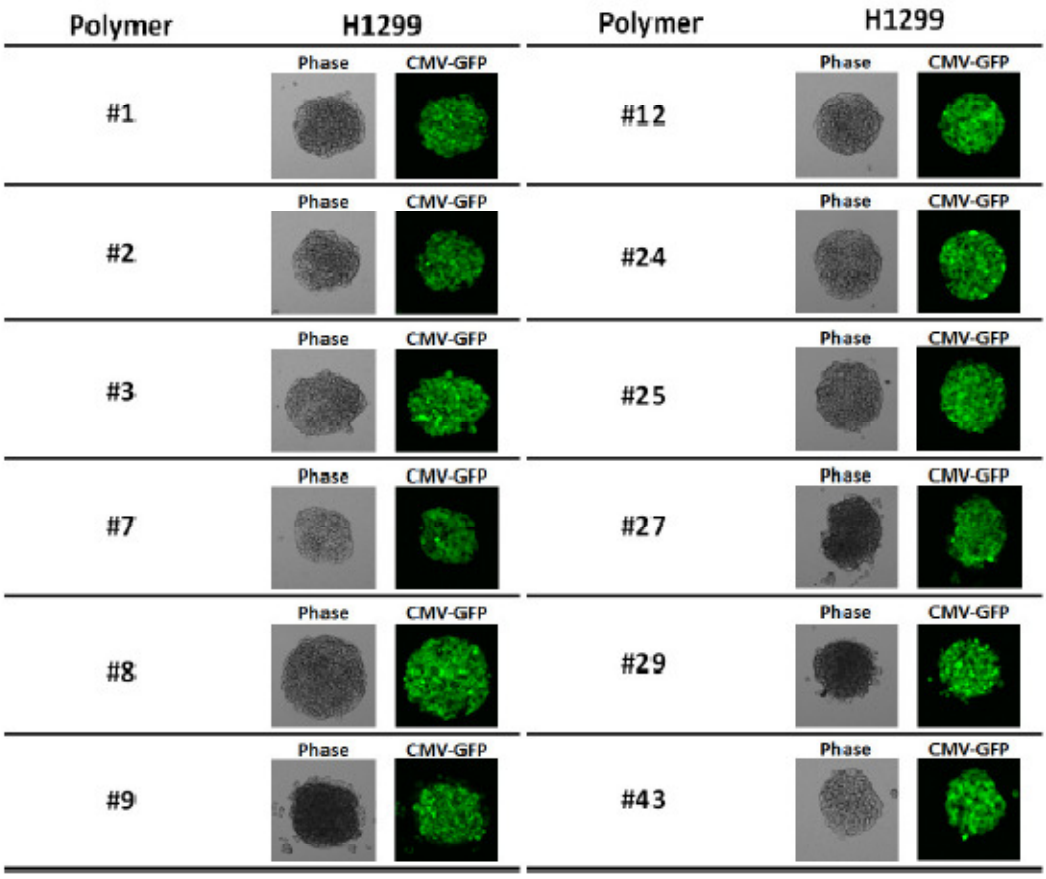

Figure 13. Polymers that support H1299 attachment/proliferation. Microarray screening of 43 polymers led to discovery of these 12 polymers as potential substrates for H1299 culture.

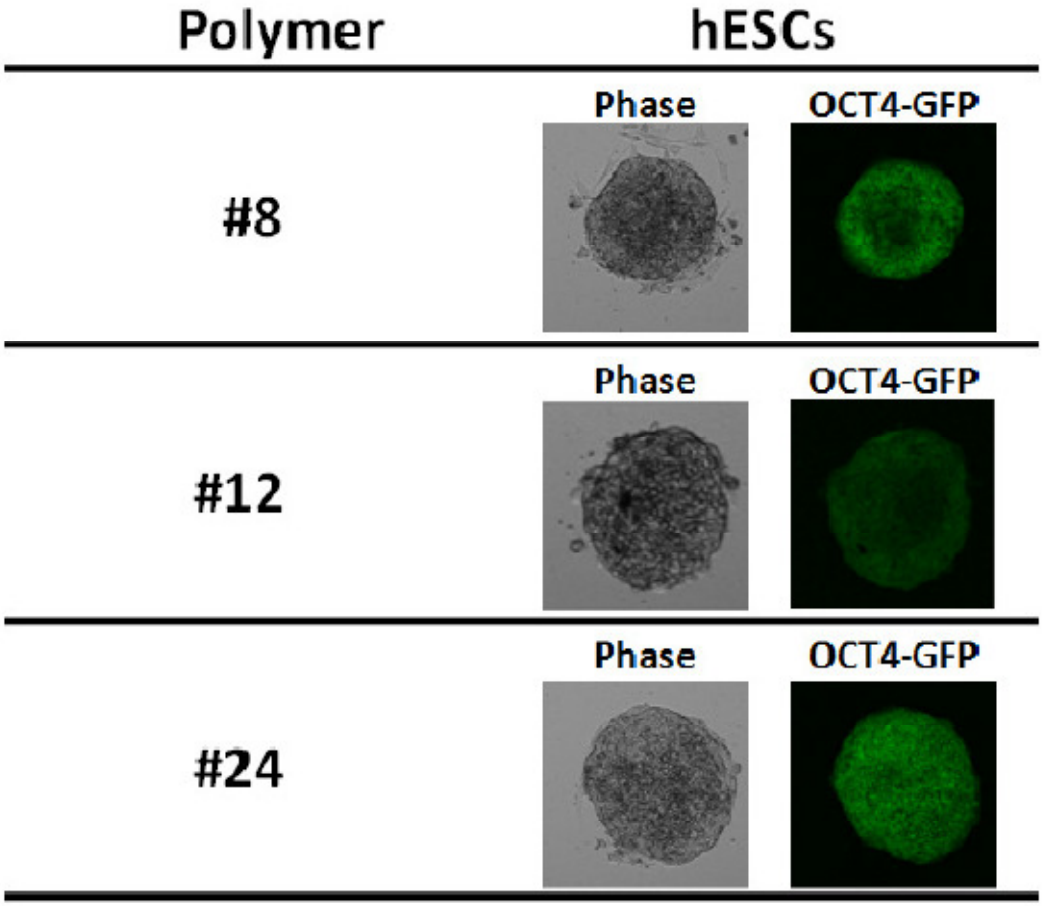

Figure 14. Polymers that support hESC attachment/proliferation. Microarray screening of 43 polymers led to discovery of Polymers #8,#12, and #24 as potential substrates for hESC culture.

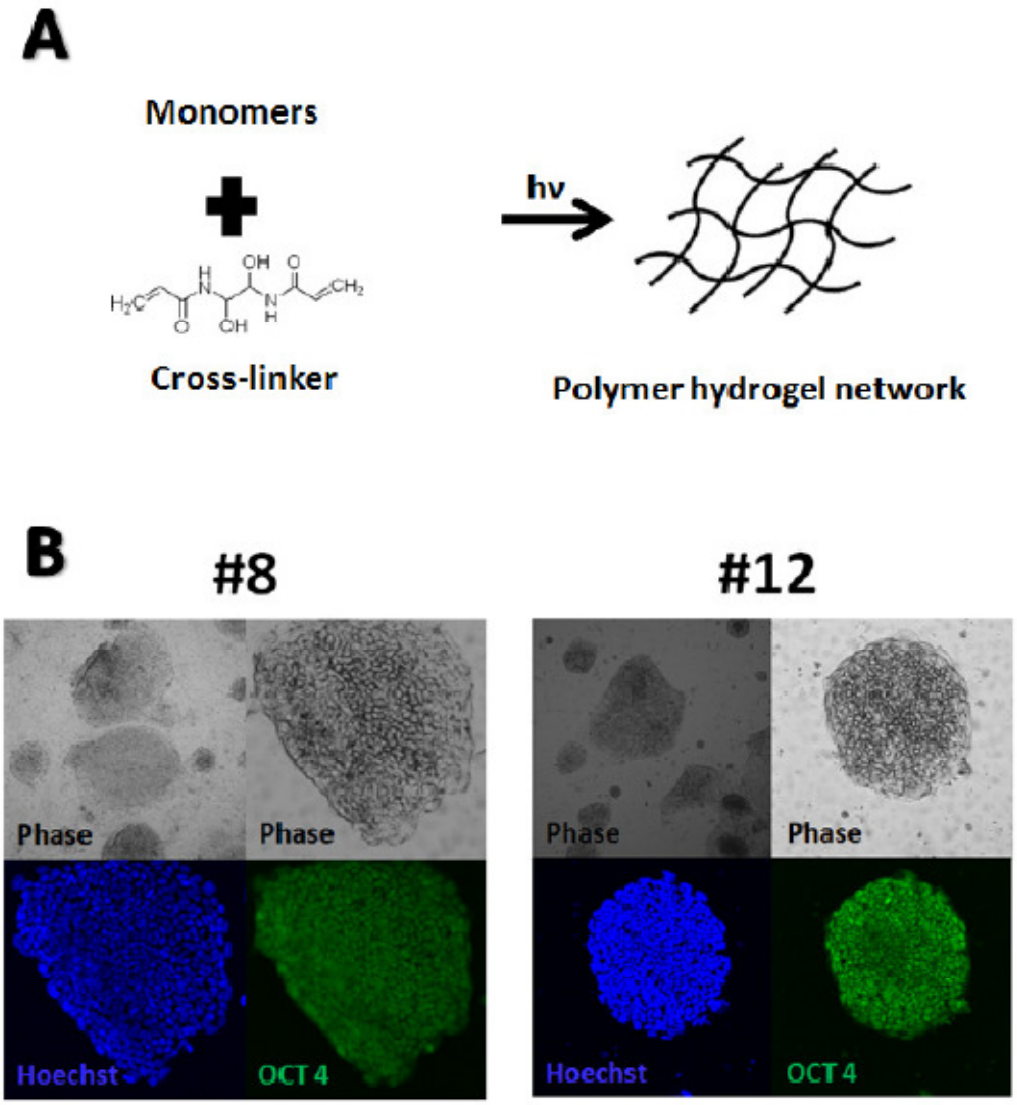

Figure 15. Polymer hydrogel formation and hESC culture. **A)** Formation of polymer hydrogels from monomers (#8 and #12) and crosslinker (bis-acrylamide) with photoinitiator during exposure to UV light. These hydrogels were created on silanized glass slides (similar to acrylamide gel pads made for microarray printing). **B)** Cells cultured on these polymers form colonies and maintain Oct-4 expression.

A

Cell Type	Percentage										
293	100	90	80	70	60	50	40	30	20	10	0
293 GFP	0	10	20	30	40	50	60	70	80	90	100

B

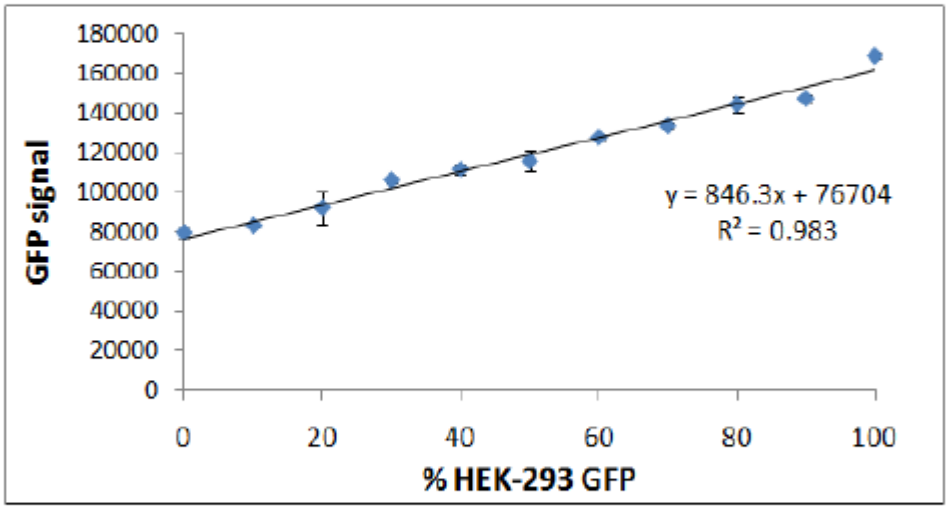

Figure 16. Development of GFP assay. A) Formation a gradient of GFP expressing cells by mixing HEK-293 GFP with HEK-293 cells. B) Plate reader assay for GFP establishing sensitivity of plate reader in detecting 10% differences in GFP signal.

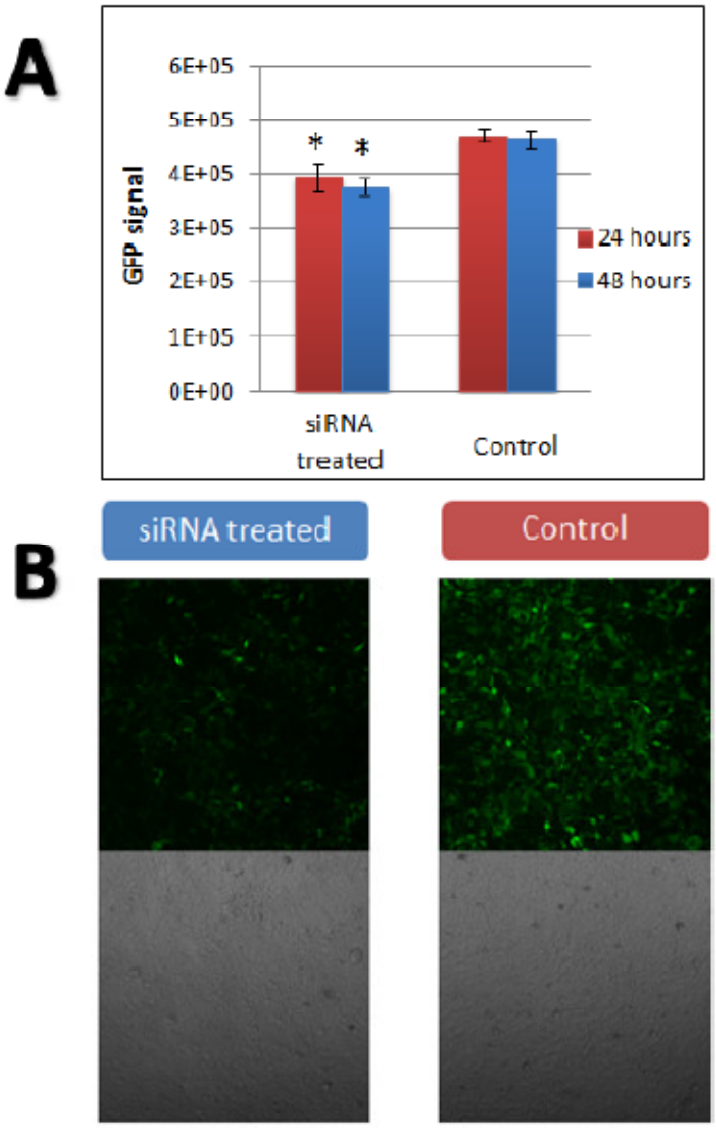

Figure 17. siRNA treatment on HEK-293 GFP cells. A) Plate reader data of siRNA treatment on HEK-293 GFP cells at 24 and 48 hour time points. B) Confocal microscope images at 24 hours after treatment.

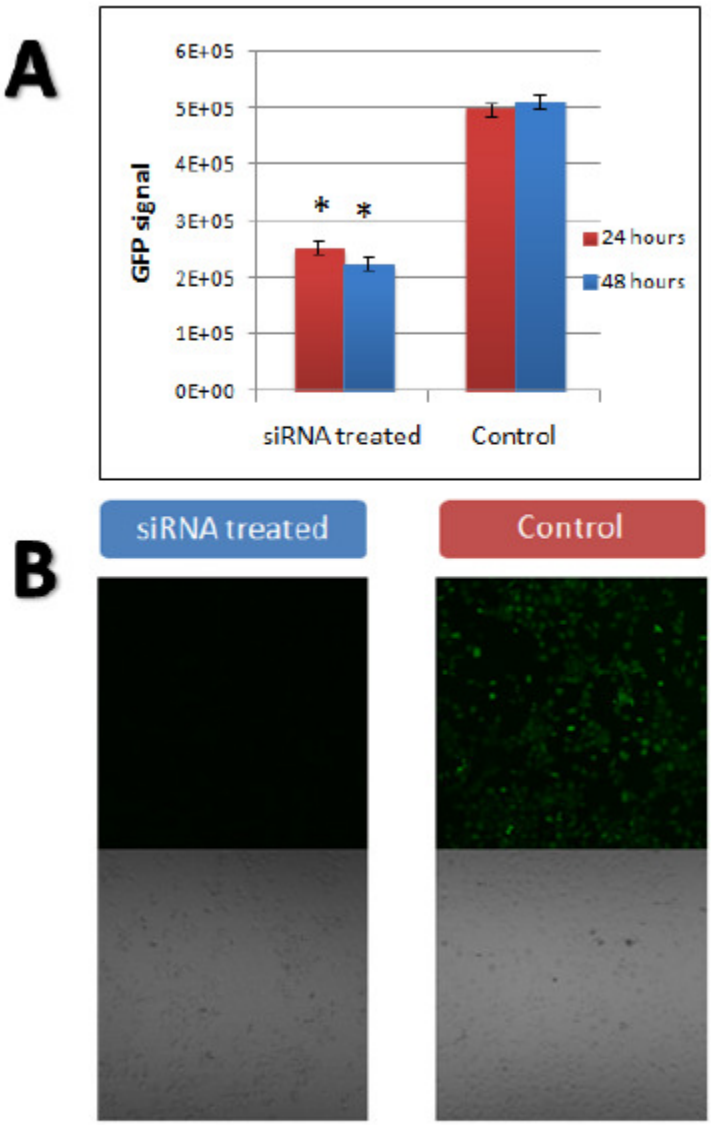

Figure 18. siRNA treatment on dGFP H1299 cells. A) Plate reader data of siRNA treatment on dGFP H1299 cells at 24 and 48 hour time points. B) Confocal microscope images at 24 hours after treatment.

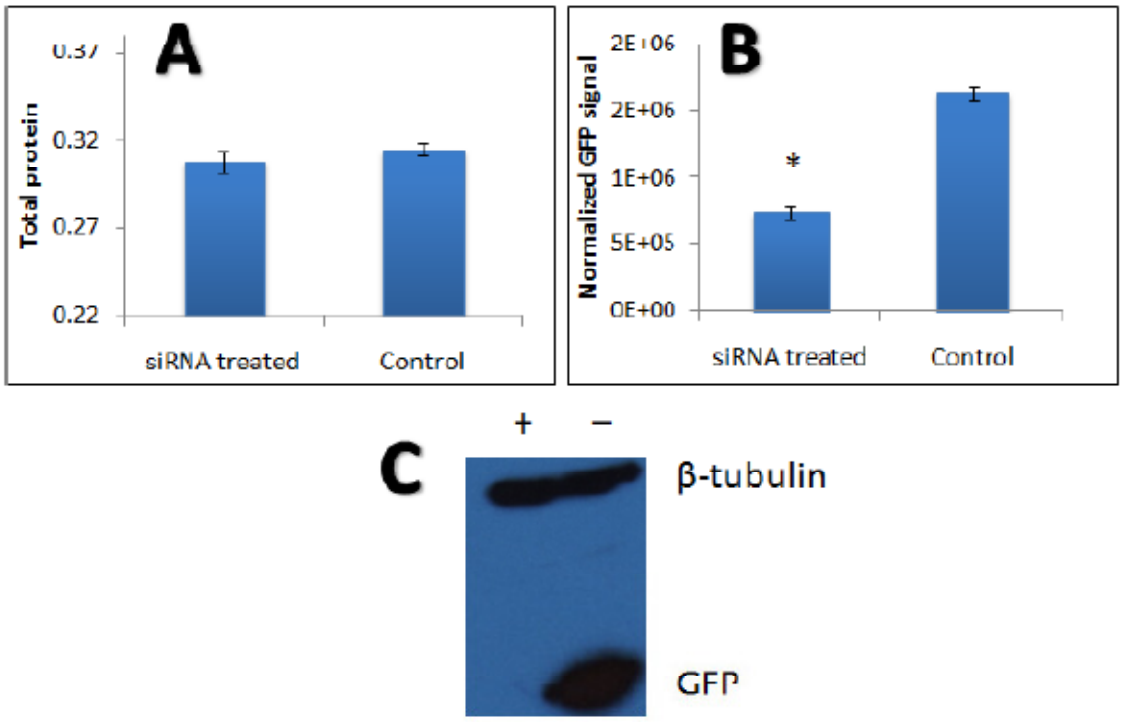

Figure 19. siRNA-induced knockdown of GFP. A) Total protein (Coommassie) at 48 hours. B) 48 hour GFP signal (from Fig. 19A) normalized by total protein (A). C) Western blot of siRNA treated (+) and control (–) dGFP H1299 cells after 48 hours.

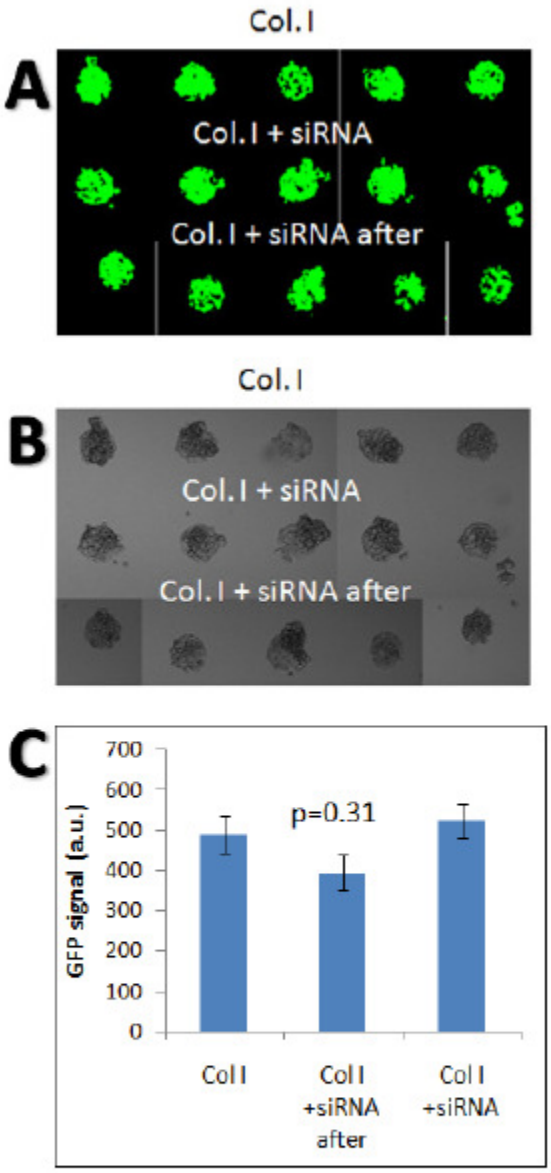

Figure 20. siRNA knockdown on microarray format. **A)** GFP expression of dGFP H1299 cells seeded on a microarray spotted with Collagen I, Collagen I and PTD-dRBD-siRNA together, and Collagen I with PTD-dRBD-siRNA spotted on top (labeled after). **B)** Corresponding phase contrast image. **C)** Image analysis of GFP expression.

Figures 1, 2, 3, and 5 are reproductions from Brafman D, Shah K, Fellner T, Chien S, Willert K. Defining long-term maintenance conditions of human embryonic stem cells with arrayed cellular microenvironment technology. Stem Cells and Development, 2009 (In Press). The thesis author was the secondary author of this paper.

REFERENCES

1. Flaim, C.J., et al., *Combinatorial signaling microenvironments for studying stem cell fate.* Stem Cells Dev, 2008. **17**(1): p. 29-39.

2. Flaim, C.J., S. Chien, and S.N. Bhatia, *An extracellular matrix microarray for probing cellular differentiation.* Nat Methods, 2005. **2**(2): p. 119-25.

3. Brafman, D.A., et al., *Defining long-term maintenance conditions of human embryonic stem cells with arrayed cellular microenvironment technology.* Stem Cells and Development, 2009(In Press).

4. Thomson, J.A., et al., *Embryonic stem cell lines derived from human blastocysts.* Science, 1998. **282**(5391): p. 1145-7.

5. Hoffman, L.M. and M.K. Carpenter, *Characterization and culture of human embryonic stem cells.* Nat Biotechnol, 2005. **23**(6): p. 699-708.

6. Skottman, H. and O. Hovatta, *Culture conditions for human embryonic stem cells.* Reproduction, 2006. **132**(5): p. 691-8.

7. Martin, M.J., et al., *Human embryonic stem cells express an immunogenic nonhuman sialic acid.* Nat Med, 2005. **11**(2): p. 228-32.

8. Xu, C., et al., *Basic fibroblast growth factor supports undifferentiated human embryonic stem cell growth without conditioned medium.* Stem Cells, 2005. **23**(3): p. 315-23.

9. Xu, C., et al., *Feeder-free growth of undifferentiated human embryonic stem cells.* Nat Biotechnol, 2001. **19**(10): p. 971-4.

10. Wang, L., et al., *Self-renewal of human embryonic stem cells requires insulin-like growth factor-1 receptor and ERBB2 receptor signaling.* Blood, 2007. **110**(12): p. 4111-9.

11. Sato, N., et al., *Maintenance of pluripotency in human and mouse embryonic stem cells through activation of Wnt signaling by a pharmacological GSK-3-specific inhibitor.* Nat Med, 2004. **10**(1): p. 55-63.

12. Ludwig, T.E., et al., *Derivation of human embryonic stem cells in defined conditions.* Nat Biotechnol, 2006. **24**(2): p. 185-7.

13. James, D., et al., *TGFbeta/activin/nodal signaling is necessary for the maintenance of pluripotency in human embryonic stem cells.* Development, 2005. **132**(6): p. 1273-82.

14. Heins, N., et al., *Derivation, characterization, and differentiation of human embryonic stem cells.* Stem Cells, 2004. **22**(3): p. 367-76.

15. Amit, M., et al., *Feeder layer- and serum-free culture of human embryonic stem cells.* Biol Reprod, 2004. **70**(3): p. 837-45.

16. Yao, S., et al., *Long-term self-renewal and directed differentiation of human embryonic stem cells in chemically defined conditions.* Proc Natl Acad Sci U S A, 2006. **103**(18): p. 6907-12.

17. Noaksson, K., et al., *Monitoring differentiation of human embryonic stem cells using real-time PCR.* Stem Cells, 2005. **23**(10): p. 1460-7.

18. Genbacev, O., et al., *Serum-free derivation of human embryonic stem cell lines on human placental fibroblast feeders.* Fertil Steril, 2005. **83**(5): p. 1517-29.

19. Braam, S.R., et al., *Recombinant vitronectin is a functionally defined substrate that supports human embryonic stem cell self-renewal via alphavbeta5 integrin.* Stem Cells, 2008. **26**(9): p. 2257-65.

20. Beattie, G.M., et al., *Activin A maintains pluripotency of human embryonic stem cells in the absence of feeder layers.* Stem Cells, 2005. **23**(4): p. 489-95.

21. Chen, S.S., et al., *Cell-cell and cell-extracellular matrix interactions regulate embryonic stem cell differentiation.* Stem Cells, 2007. **25**(3): p. 553-61.

22. Campbell, A., M.S. Wicha, and M. Long, *Extracellular matrix promotes the growth and differentiation of murine hematopoietic cells in vitro.* J Clin Invest, 1985. **75**(6): p. 2085-90.

23. Adewumi, O., et al., *Characterization of human embryonic stem cell lines by the International Stem Cell Initiative.* Nat Biotechnol, 2007. **25**(7): p. 803-16.

24. *Denaturing Agarose Gel Electrophoresis of RNA*. 11-11-2008]; Available from: http://www.ambion.com/techlib/append/supp/rna_gel.html.

25. Nichols, J., et al., *Formation of pluripotent stem cells in the mammalian embryo depends on the POU transcription factor Oct4.* Cell, 1998. **95**(3): p. 379-91.

26. Chambers, I., et al., *Functional expression cloning of Nanog, a pluripotency sustaining factor in embryonic stem cells.* Cell, 2003. **113**(5): p. 643-55.

27. Stojkovic, P., et al., *Human-serum matrix supports undifferentiated growth of human embryonic stem cells.* Stem Cells, 2005. **23**(7): p. 895-902.

28. Streuli, C., *Extracellular matrix remodelling and cellular differentiation.* Curr Opin Cell Biol, 1999. **11**(5): p. 634-40.

29. Spradling, A., D. Drummond-Barbosa, and T. Kai, *Stem cells find their niche.* Nature, 2001. **414**(6859): p. 98-104.

30. Saltzman, W.M., *Cell Interactions with Polymers*, in *Principles of Tissue Engineering*. 2000, Academic Press: San Diego. p. 221-235.

31. Meredith, J.C., et al., *Combinatorial characterization of cell interactions with polymer surfaces.* J Biomed Mater Res A, 2003. **66**(3): p. 483-90.

32. Wojciak-Stothard, B., et al., *Activation of macrophage-like cells by multiple grooved substrata. Topographical control of cell behaviour.* Cell Biol Int, 1995. **19**(6): p. 485-90.

33. Ranucci, C.S. and P.V. Moghe, *Polymer substrate topography actively regulates the multicellular organization and liver-specific functions of cultured hepatocytes.* Tissue Eng, 1999. **5**(5): p. 407-20.

34. Meyle, J., H. Wolburg, and A.F. von Recum, *Surface micromorphology and cellular interactions.* J Biomater Appl, 1993. **7**(4): p. 362-74.

35. Huang, S. and D.E. Ingber, *Shape-dependent control of cell growth, differentiation, and apoptosis: switching between attractors in cell regulatory networks.* Exp Cell Res, 2000. **261**(1): p. 91-103.

36. Hannon, G.J., *RNA interference.* Nature, 2002. **418**(6894): p. 244-51.

37. Fire, A., et al., *Potent and specific genetic interference by double-stranded RNA in Caenorhabditis elegans.* Nature, 1998. **391**(6669): p. 806-11.

38. Meister, G. and T. Tuschl, *Mechanisms of gene silencing by double-stranded RNA.* Nature, 2004. **431**(7006): p. 343-9.

39. Bernstein, E., A.M. Denli, and G.J. Hannon, *The rest is silence.* RNA, 2001. **7**(11): p. 1509-21.

40. Alberts, B., Johnson, A., Lewis, J., Raff, M., Roberts, K., Walter, P., *Molecular Biology of the Cell*. 5 ed. 2008, New York: Garland Science.

41. Poulin, G., R. Nandakumar, and J. Ahringer, *Genome-wide RNAi screens in Caenorhabditis elegans: impact on cancer research.* Oncogene, 2004. **23**(51): p. 8340-5.

42. Ganesan, A.K., et al., *Genome-Wide siRNA-Based Functional Genomics of Pigmentation Identifies Novel Genes and Pathways That Impact Melanogenesis in Human Cells.* PLoS Genet, 2008. **4**(12): p. e1000298.

43. Berns, K., et al., *A large-scale RNAi screen in human cells identifies new components of the p53 pathway.* Nature, 2004. **428**(6981): p. 431-7.

44. Behlke, M.A., *Progress towards in vivo use of siRNAs.* Mol Ther, 2006. **13**(4): p. 644-70.

45. *Traversa's RNAi Delivery Technology: PTD-DRBD*. 2008 [cited 2008 2/20]; Available from: http://www.traversathera.com/rnai_delivery_detail.php.

46. Frankel, A.D. and C.O. Pabo, *Cellular uptake of the tat protein from human immunodeficiency virus.* Cell, 1988. **55**(6): p. 1189-93.

47. Vives, E., P. Brodin, and B. Lebleu, *A truncated HIV-1 Tat protein basic domain rapidly translocates through the plasma membrane and accumulates in the cell nucleus.* J Biol Chem, 1997. **272**(25): p. 16010-7.